universität wien

DIPLOMARBEIT

Titel der Diplomarbeit

Subcellular Localisation and Function of the
Calcium-Dependent Protein Kinase CPK3
in *Arabidopsis thaliana*

angestrebter akademischer Grad

Magistra der Naturwissenschaften (Mag. rer.nat.)

Verfasserin / Verfasser:	Barbara Pfister
Studienrichtung /Studienzweig (lt. Studienblatt):	Molekulare Biologie, A490
Betreuerin / Betreuer:	Dr. Markus Teige

Wien, im Dezember 2010

Danksagung

Mein größter Dank gilt Markus Teige. Danke für das interessante Projekt, die hervorragende Betreuung und das Vertrauen in mich und meine Fähigkeiten.

Ich möchte auch meinen Kollegen Bernhard, Simon und Andrea danken, die mir stets mit Rat und Tat zur Seite gestanden sind und mit denen ich auch zahlreiche heitere Stunden außerhalb des Labor 1 verbracht habe. Dank euch bin ich auch in schwierigeren Zeiten immer gerne ins Labor gegangen.

Danke an meine Familie, Mama und Papa, Ingrid und Angie, ohne eure Unterstützung wäre mein Studium nicht möglich gewesen. Ich möchte mich auch bei Inge bedanken, die mir in unseren Gesprächen oft einen anderen Blick auf wissenschaftliche Themen ermöglicht hat.

Zu guter Letzt danke ich Simon. Danke, dass du für mich da warst, wenn ich dich gebraucht habe.

Zusammenfassung

Pflanzen sind einer Vielzahl von schädlichen Umweltbedingungen wie salzhaltigen Böden, Kälte oder Pathogenen ausgesetzt. Um diesen Einflüssen standzuhalten, haben sie faszinierende Abwehrmechanismen entwickelt. Am Beginn solcher Anpassungen stehen meist lokal begrenzte Ca^{2+}-Signale, die von Ca^{2+}-bindenden Sensoren erfasst und in eine zelluläre Antwort umgewandelt werden.

CPK3 ist Teil der konservierten Familie der kalziumabhängigen Proteinkinasen (CDPKs), die durch Ca^{2+} aktiviert werden und häufig in Stressantworten involviert sind. Kürzlich wurde gezeigt, dass CPK3 in der Modellpflanze *Arabidopsis thaliana* essentiell für die Anpassung an Salzstress ist (Mehlmer *et al.*, 2010). Die genaue Funktion von CPK3 ist jedoch noch unbekannt.

Das Ziel meiner Arbeit war es, die subzelluläre Lokalisierung von CPK3 zu untersuchen, um Hinweise auf die Funktion dieser Kinase zu erhalten. Ich war insbesondere an ihrer Membranassoziierung interessiert, da CPK3 wahrscheinlich an der Regulierung von membranständigen Ionenkanälen beteiligt ist (Mori *et al.*, 2006), was auch ihre Rolle im Salzstress erklären könnte. Mithilfe von biochemischen Methoden konnte ich zeigen, dass CPK3 eine gewebespezifische Lokalisierung aufweist: Während CPK3 in Blättern sowohl mit der Plasmamembran als auch mit der vakuolären Membran assoziiert ist, ist sie in Wurzeln wahrscheinlich ausschließlich in der Plasmamembran verankert. Dies deutet auf unterschiedliche Funktionen und Interaktionspartner von CPK3 in diesen zwei Organen hin.

Außerdem habe ich Proteine, die zuvor als mögliche Substrate von CPK3 identifiziert worden waren (Mehlmer *et al.*, 2010), auf ihre Interaktion mit CPK3 hin getestet. Anhand von Bimolekularer Fluoreszenzkomplementation (BiFC) konnte ich zeigen, dass u.a. ein Remorin, ERD13 und zwei Phosphatasen aus der PP2C-Familie mit CPK3 *in vivo* interagieren und somit interessante Objekte für weitere Analysen darstellen.

Mithilfe dieser Technik konnte ich auch nachweisen, dass TPK1, ein vakuolärer K^+-Kanal, mit CPK3 *in planta* interagiert. Die Mutation zweier Arginine in der Interaktionsdomäne von TPK1 verringerte die Interaktion in signifikantem Ausmaß, was die Spezifität der beobachteten Interaktion demonstriert. Durch die Verwendung von Keimungsexperimenten konnte ich außerdem zeigen, dass sowohl TPK1 als auch CPK3 wichtig für die K^+-Homöostase bei Salzstress sind. Dies bedeutet, dass die mögliche Regulation von TPK1 durch CPK3 einen Mechanismus darstellen könnte, der erklärt, wie CPK3 die Toleranz von Pflanzen gegenüber Salzstress erhöht.

Abstract

Plants are exposed to a variety of hostile environmental factors, such as soil salinity, cold or pathogens. In order to cope with these conditions, they have evolved fascinating defence mechanisms. A rise in cytosolic Ca^{2+} levels is often the beginning of stress responses. These locally restricted signals are sensed by Ca^{2+} binding proteins, which translate the signals into a cellular response.

CPK3 belongs to the family of Ca^{2+}-dependent protein kinases, which are activated upon binding of Ca^{2+}. It has recently been shown in our lab that CPK3 is required for salt-stress acclimation in the model plant *Arabidopsis thaliana* (Mehlmer *et al.*, 2010). The precise function of CPK3, however, has not been elucidated yet.

The aim of my work was to analyse the subcellular localisation of CPK3 in order to gain insights into the functions of this kinase. In particular, I was interested in the membrane association of CPK3, as a regulation of ion channels by CPK3 has been proposed previously by Mori *et al.* (2006). Using biochemical approaches, I was able to show that CPK3 displays a tissue-specific localisation. Whereas CPK3 is associated with the plasma membrane and the vacuolar membrane in leaves, my data indicate that it is exclusively attached to the plasma membrane in roots. This suggests that CPK3 has different functions and molecular targets in these two organs.

In addition, I tested proteins which had been identified as putative targets of CPK3 by phosphoproteomics (Mehlmer *et al.*, 2010) for their interaction with CPK3. Bimolecular fluorescence complementation (BiFC) revealed that a remorin protein, ERD13 and two PP2C-type phosphatases interact with CPK3 *in vivo*. Accordingly, these proteins are interesting objects for further analysis.

Using BiFC, I could furthermore show that the vacuolar K^+ channel TPK1 interacts with CPK3 *in planta* as well. Mutation of two arginines in the predicted interaction domain of TPK1 resulted in a significantly reduced signal, demonstrating the specificity of the observed interaction. Germination assays revealed that both TPK1 and CPK3 are important for K^+ homeostasis under salt stress. Thus, the regulation of TPK1 by CPK3 provides a mechanism that explains how CPK3 may increase the tolerance of plants towards salt stress.

Contents

1 Introduction

1.1 Plants in the Response to Salt Stress

Plants are exposed to a persistently changing and often inhospitable environment. In order to survive and reproduce, they need to cope with diverse environmental factors, such as cold, drought, salinity or strong light (Hirayama and Shinozaki, 2010). Among these, soil salinity is one of the most abundant abiotic stresses, which affects more than 20% of irrigated land and reduces crop productivity substantially (Munns and Tester, 2008).

An increased concentration of salt in the soil imposes two major constraints to plants: First, it impedes the uptake of water from the soil, and second, it leads to higher levels of Na^+ within the plants, which may be toxic, e.g. by inhibiting enzyme activities (Munns and Tester, 2008; Shabala and Cuin, 2007). The first component is referred to osmotic stress, the latter to ionic stress (Munns and Tester, 2008). To face these impacts of salt stress, plants have evolved several mechanisms, including the active export of Na^+ from roots back to the soil, its extrusion out of the xylem, by which it would be transported to the leaves, and its sequestering into the vacuole both in roots and leaves (Munns and Tester, 2008). These measures require the concerted action of ion channels and transporters such salt overly sensitive 1 (SOS1), Na^+ transporters of the high-affinity K^+ transporter (HKT) family and members of the Na^+/H^+ exchanger family (NHX) (Munns and Tester, 2008; Horie *et al*., 2006; Sunarpi *et al*., 2005).

Another negative effect of soil salinity is its implication for mal-nutrition of plants (Shabala and Cuin, 2007). In particular, salt stress hampers the uptake of K^+ from the soil, favouring K^+ deficiency (Shabala and Cuin, 2007). This is problematic, as a high K^+/Na^+ ratio in the cytosol is needed to confine the toxic capacity of Na^+ by competing with K^+ for binding sites at enzymes (Shabala and Cuin, 2007; Obata *et al.*, 2007). Moreover, K^+ is an important osmolyte that counteracts the loss of osmotic pressure in the cytosol due to the sequestration of Na^+ into the vacuole (Munns and Tester, 2008). Although compatible solutes such as sucrose, proline or glycine betaine contribute to this as well, the biosynthesis of these consumes huge amounts of ATP and should therefore be rather avoided (Shabala and Cuin, 2007; Munns and Tester, 2008). Accordingly, K^+ transporters and K^+ permeable channels such as KUP/HAK/KT transporters, AKT2/3 and TPKs play important roles in salt-stress acclimation as well and need to be investigated in order to understand these mechanisms of salinity tolerance (Shabala and Cuin, 2007).

1.2 Ca^{2+} as a Ubiquitous Second Messenger

Ca^{2+} signals are elicited by a plethora of extracellular stimuli such as fungal elicitors, cold, drought or salt stress (Sanders *et al*., 1999). In the salt stress response, increasing Ca^{2+} influx into the cytosol of root cells is one of the first known changes and triggers the activation of SOS1, a Na^+/H^+ antiporter identified by Shi *et al.* (2000) that is localised in the plasma membrane and extrudes Na^+ back to the soil (Munns and Tester, 2008). Besides being involved in diverse stress responses (Kiegle *et al.*, 2000; Zhang *et al.*, 2009; Haley *et al.*, 1995), Ca^{2+} is also implicated in the establishment of symbiosis with rhizobia and mycorrhizal fungi (Shaw and Long, 2003; Kosuta *et al.*, 2008) as well as in the tip growth of pollen tubes and root hair cells (Hepler *et al.*, 2001; Kudla *et al.*,2010). Two interesting features have paved the way for Ca^{2+} to become so important: First, it easily forms precipitates with ions such as phosphate, which demands very low cytosolic Ca^{2+} concentrations of approximately 200 nM (Sanders *et al.*, 1999; Kudla *et al.*, 2010). This has favoured the evolution of effective Ca^{2+} exporters and enables small influxes of Ca^{2+} to change its cytosolic concentration several-fold (Kudla *et al.*, 2010; Sanders *et al*., 1999).

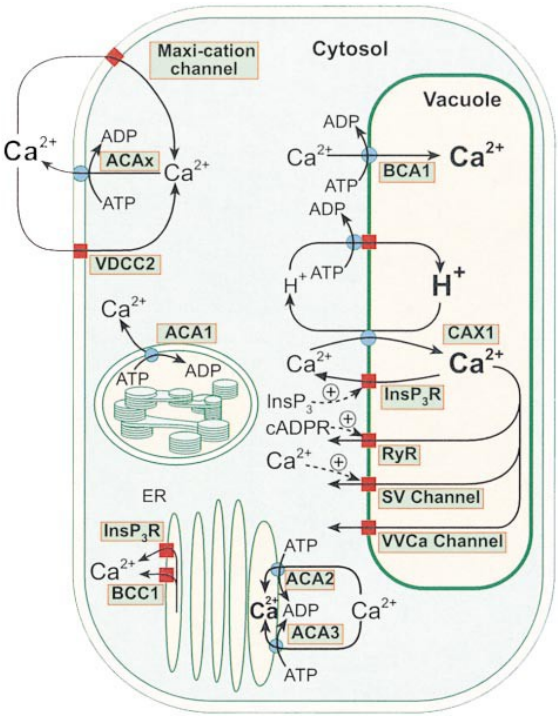

Figure 1.2.1. Ca^{2+} transport pathways in plant cells. Energised transport systems are shown as blue circles, red squares represent Ca^{2+} ion channels. ACAx, autoinhibited Ca^{2+}-ATPase isoform x; BCC1, *Brionica* Ca^{2+} channel; CAX, cation exchanger; $InsP_3R$, putative $InsP_3$ receptor; RyR, putative ryanodine receptor; SV channel, slowly activating vacuolar channel; VDCC2, voltage-dependent Ca^{2+} channel 2; VVCa channel, vacuolar voltage-gated Ca^{2+} channel (Sanders *et al.*, 1999).

Second, Ca^{2+} can be chelated by a considerable number of uncharged oxygen atoms, allowing for conformational changes in these proteins upon Ca^{2+} binding (Kudla *et al.*, 2010; Sanders *et al*., 1999).

The fact that Ca^{2+} is implicated in a plethora of cellular responses raises the question how specificity is established (Sanders *et al.*, 1999). It has been shown that Ca^{2+} signals differ in their amplitude, duration and frequency (Sanders *et al*., 1999). In addition, Ca^{2+} signals arise at distinct cellular locations (Sanders *et al.*, 1999). This is established by Ca^{2+}-permeable ion channels located at the diverse Ca^{2+} stores in the cell, such as the vacuole, the endoplasmic reticulum (ER), the chloroplast, the mitochondria, the nuclear envelope, and the apoplast (Fig. 1.2.1; Cheng *et al.*, 2002; Sanders *et al.*, 1999). This spacio-temporal regulation of Ca^{2+} signals has led to the idea of "Ca^{2+} signatures" (Webb *et al*., 1996; Kudla *et al.*, 2010). Another layer of specificity is provided by the set of Ca^{2+} sensing proteins, which varies depending on cell type and developmental stage (Sanders *et al.*, 1999; Kudla *et al.*, 2010). For guard cells, in which Ca^{2+} is involved in both stomatal closure *and* opening, the Ca^{2+} priming model has been formulated by Young and co-workers (2006) to provide an additional mechanism for specificity (Kudla *et al*., 2010). In this model, extracellular stimuli such as low CO_2 or ABA do not only induce Ca^{2+} spiking but also modulate the sensitivity of Ca^{2+} sensors to favour distinct signalling pathways (Young *et al.*, 2006). As an evidence for this, Siegel and co-workers have recently shown that ABA increases the activation of S-type anion channels upon Ca^{2+} signals (Siegel *et al*., 2009; Kudla *et al.*, 2010).

1.3 Ca^{2+}-Regulated Proteins

Decoding of Ca^{2+} signals is performed by a plethora of proteins that can be divided into sensor relays and sensor responders (Kudla *et al.*, 2010). Sensor relays are able to bind Ca^{2+} but do not exhibit a catalytic function. This group includes the family of calmodulins (CaM) and calcineurin B-like proteins (CBLs), which bind to and thereby relay a conformational change to interacting effector proteins (Kudla *et al.*, 2010). In contrast, Ca^{2+} sensor responders combine binding of Ca^{2+} and catalytic activity within a single polypeptide (Kudla *et al*., 2010). In plants, this group is represented by the family of calcium-dependent protein kinases (CDPKs).

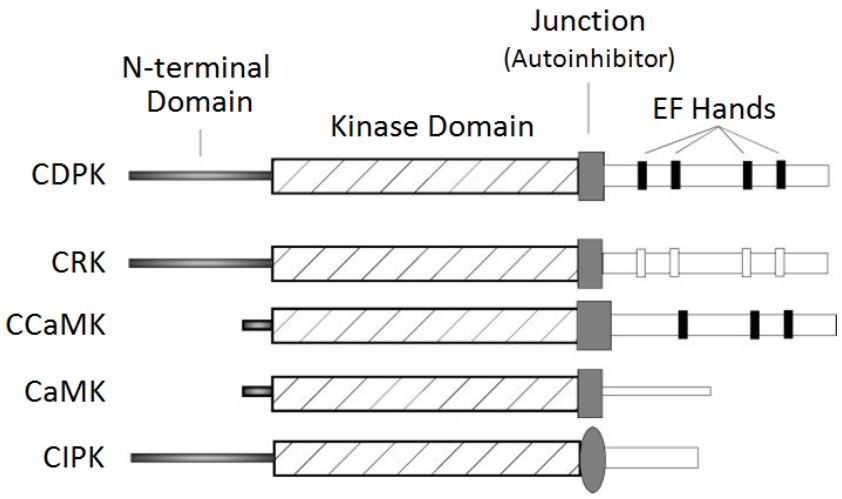

Figure 1.3.1. Structures of Ca^{2+}-regulated protein kinases. The shaded boxes show the autoinhibitory region of CDPKs or related regions in other kinases. EF hands are depicted in black, degenerated EF hands in white. CDPK, Ca^{2+}-dependent protein kinase; CRK, CDPK-related kinase; CCaMK, Ca^{2+}- and calmodulin-activated protein kinase; CaMKs, calmodulin-dependent protein kinase; CIPK, CBL- (Calcineurin-B like) interacting protein kinase (adapted from Harper *et al*., 2004).

Among the Ca^{2+}-regulated proteins, kinases are the most important group. These proteins translate Ca^{2+} signals into a cellular response by phosphorylating effector proteins such as transcription factors or ion channels (Dodd *et al*., 2010). Besides CDPKs, Ca^{2+} regulated protein kinases include (i) CDPK-related kinases (CRKs), which have degenerated EF hands and may be activated by binding to CaM; (ii) calmodulin-dependent protein kinases (CaMKs); (iii) Ca^{2+}- and calmodulin-activated kinases (CCaMKs), and CBL-interacting protein kinases (CIPKs) (Fig. 1.3.1; Harper *et al*., 2004). Whereas the *Arabidopsis* genome encodes 34 CDPKs, 26 CIPKs, and eight CRKs, neither CaMKs nor CCaMKs have been identified in this organism (Harper *et al*., 2004; Kudla *et al*., 2010). Nevertheless, these Ca^{2+}-regulated kinases are not fully absent in plants, as apple has a CaMK and CCaMKs have been found in other model plants, such as in tobacco, rice and *Physcomitrella* (Harper *et al*., 2004).

There are also transcription factors that are activated by binding to calmodulin (Kudla *et al.*, 2010). These proteins constitute the family of Ca^{2+}-dependent calmodulin binding transcription factors (CAMTAs), of which six have been identified in *Arabidopsis* (Buche *et al*., 2002; Finkler, *et al*., 2007). In addition, it has recently been shown that the calmodulin AtCAM7 directly acts as a transcriptional regulator, implying that this is another Ca^{2+} sensor responder in plants (Kushwaha *et al.*, 2008; Kudla *et al.*, 2010).

1.4 Calcium-Dependent Protein Kinases

Calcium-dependent protein kinases constitute a well-characterised family of Ser/Thr protein kinases, which is expressed ubiquitously throughout the plant kingdom and in some protozoans such as *Plasmodium falciparum*, but not in animals or fungi (Cheng *et al.*, 2002; Zhao *et al.*, 1994). For instance, 29 CDPKs have been identified in rice and 34 in *Arabidopsis thaliana*, constituting approximately half the kinases implicated in Ca^{2+} signalling in *A. thaliana* (Witte *et al.*, 2010; Harper *et al.*, 2004). The overall identity of *Arabidopsis* CDPKs ranges between 39% and 95%, which has led to the division into four subgroups corresponding to their relatedness (Fig. 1.4.1; Cheng *et al.*, 2002).

As shown in figure 1.3.1, CDPKs contain four domains: (i) an N-terminal variable domain, which contains information for subcellular targeting and substrate specificity; (ii) a highly conserved protein kinase domain; (iii) an autoinhibitory region, which inhibits kinase activity if the appropriate Ca^{2+} signal is absent; and (iv) a calmodulin-like domain with one to four EF hands, which binds to Ca^{2+} (Cheng *et al.*, 2002). In recent literature, the autoinhibitory region and the CaM-like domain together are termed the C-terminal CDPK activation domain (e.g. in Wernimont *et al.*, 2010). The structural features of a CDPK allow the combination of a certain Ca^{2+} activation threshold with a distinct kinase specificity (Harper *et al.*, 2004) and also cotargeting of Ca^{2+} sensing and enzymatic function to distinct subcellular locations, thus rendering CDPKs important switches in transduction of Ca^{2+} signals.

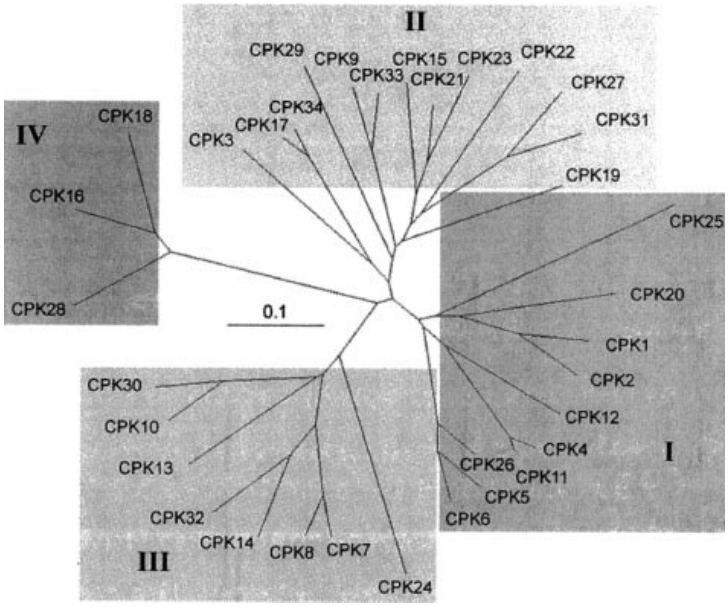

Figure 1.4.1. Sequence homologies of *Arabidopsis* CDPKs. A stretch of "0.1" refers to 10% change (Cheng *et al.*, 2002).

1.5 Regulation of CDPK Activity

Various studies have attemped to elucidate how CDPKs are activated by Ca^{2+} (e.g. Huang *et al.*, 1996; Vitart *et al.*, 2000; Chandran *et al.*, 2006). However, the major breakthrough came with the recent decipherment of crystal structures from active and inactive CDPKs in the protozoan parasites *Toxoplasma gondii* and *Cryptosporidium parvum* (Wernimont *et al.*, 2010). In its inactive form (i.e. in the absence of Ca^{2+}), the C-terminal CDPK activation domain (CAD) is built up by a long amphiphatic helix CH1 (containing the autoinhibitory region), by the N-terminal EF lobe, a shorter helix CH2 and the C-terminal EF lobe (Fig. 1.5.1A; Wernimont *et al.*, 2010). At least four regions in the CAD contribute to its binding to the kinase domain in the inactive state, most importantly a basic residue (Lys or Arg) exposed from the autoinhibitory region that bonds to an acidic cluster (Glu and Asp) in the kinase domain (Fig. 1.5.1A, Wernimont *et al.*, 2010). This Lys/Arg-Glu-Asp triad is also highly conserved in plants (Wernimont *et al.*, 2010).

Upon rise of Ca^{2+} levels, all four EF hands bind Ca^{2+}, which leads to their opening and exposure of hydrophobic regions that interact with the now partially unwound helices CH1 and CH2 (Fig. 1.5.1B, Wernimont *et al.*, 2010). In the course of this refolding, residues in the kinase domain required for substrate recognition are set free, enabling kinase activity (Wernimont *et al.*, 2010). Interestingly, the lysine residue previously bound to Glu and Asp now binds to the backbone of a Leu in the N-terminal variable domain (Wernimont *et al.*, 2010). This implies that this domain is also involved in the activation of CDPKs (Wernimont *et al.*, 2010). Despite this advance in understanding the activation of CDPKs by Ca^{2+}, it remains unclear to which extent this model can be applied to other CDPKs, in particular to cases of CDPKs having only one to three EF hands instead of four (e.g. AtCPK23 or AtCPK25, according to Cheng *et al.*, 2002).

Besides Ca^{2+}, other factors are involved in the regulation of CDPKs, including phosphorylation, binding to phospholipids and to 14-3-3 proteins (Cheng *et al.*, 2002). Although autophosphorylation is a common feature of CDPKs, its biological function remains unclear (Cheng *et al.*, 2002). In *Plasmodium falciparum* CDPK4, substitution of Thr234 in the activation loop of the kinase domain by alanine prevents not only autophosphorylation, but also blocks kinase activity, suggesting that autophosphorylation is required for catalytic activity of PfCDPK4 (Ranjan *et al.*, 2009). However, autophosphorylation in the activation loop has not been observed in a number of other CDPKs including AtCPK1 (Hegeman *et al.*, 2006; Ranjan *et al.*, 2009).

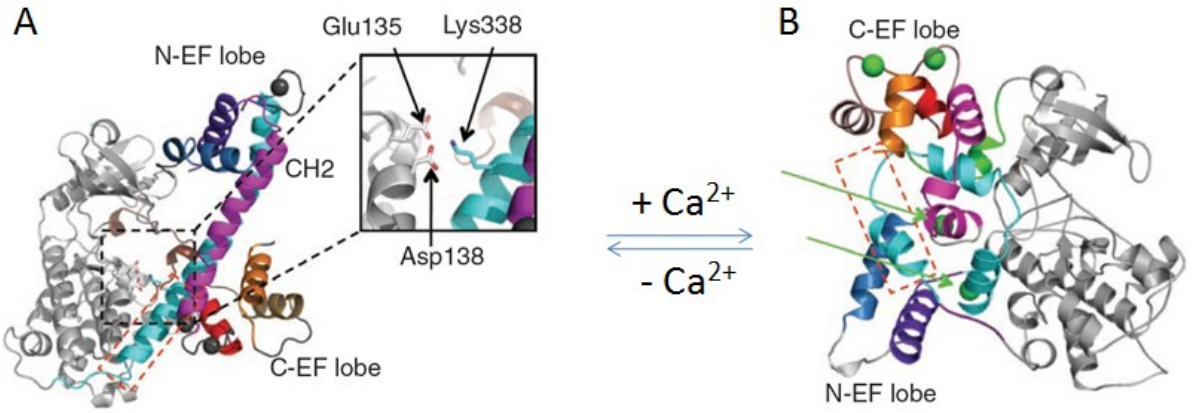

Figure 1.5.1. Crystal structures of the inactive (A) and active (B) TgCDPK3. The CAD is shown in colour and the kinase domain in grey. The CH1 and CH2 are depicted in cyan and lilac, respectively. Ca^{2+} and ions of unknown identity are shown as green or black spheres, respectively. The autoinhibitory region is framed in a red box, and the pseudosubstrate autoinhibitory triad is highlighted in black. CAD, C-terminal CDPK activation domain; N-EF lobe, N-terminal EF lobe; C-EF lobe, C-terminal EF-lobe (adapted from Wernimont *et al.*, 2010).

Phosphorylation of CDPKs by other kinases may regulate kinase activity as well. Upon mild hypo-osmotic or biotic stress, NtCDPK2 undergoes a transient conversion into an active form that exhibits 10- to 200-fold kinase activity towards the peptide substrate syntide-2 (Romeis *et al.*, 2001). Phosphatase treatment reduces this effect substantially, suggesting that phosphorylation is involved in the activation. This phosphorylation is performed most likely by an upstream kinase, as autophosphorylation of the non-elicited form did not increase its kinase activity (Romeis *et al.*, 2001). Recently, two stress-responsive *in vivo* phosphorylation sites of NtCDPK2 have been identified at its N-terminal domain (Witte *et al.*, 2010). Surprisingly, neither substitution of these two sites by alanine (impeding phosphorylation) nor aspartate (mimicking phosphorylation) changes kinase activities in vitro (Witte *et al.*, 2010). This indicates either that the identified phosphorylation sites are not the relevant ones for activation of NtCDPK2 or that the previous results need to be re-evaluated.

1.6 Localisation of CDPKs - the Effect of Fatty Acylation

CDPKs display a great variety in subcellular distribution, including cytosolic and nuclear localisation (e.g. AtCPK4), attachment to the plasma membrane (e.g. AtCPK7, AtCPK8, AtCPK9), to the ER (AtCPK2), and to peroxisomes (AtCPK1; Dammann *et al.*, 2003; Lu and Hrabak, 2002; Benetka *et al.*, 2008). In many cases, it has been shown that the targeting

signal is encoded in the N-terminal domain by the presence or absence of acylation sites, i.e. sites for *N*-myristoylation or palmitoylation (e.g. Mehlmer, 2010; Lu and Hrabak, 2002). *N*-myristoylation is the attachment of myristic acid, a C-14 saturated fatty acid, to the penultimate glycine by an *N*-myristoyltransferase (NMT) (Resh, 1999). This modification is generated co-translationally, involves the cropping of the initiating Met and is irreversible (Resh, 1999). In contrast, in palmitoylation the C-16 saturated fatty acid palmitate is linked to a cysteine via a thioester bond by a palmitoyl acyltransferase (PAT). Since palmitate can be cleaved by protein palmitoyl thioesterases, this reaction is reversible (Resh, 1999). Although palmitoylated cysteines may occur throughout the whole protein in general, in CDPKs these cysteines have been identified in the N terminus. Interestingly, 29 of the 34 CDPKs in *Arabidopsis* contain a glycine in position two, i.e. a potential myristoylation site (Benetka *et al.*, 2008), and only one of these kinases does not have a close cysteine that may be palmitoylated (AtCPK3; Cheng *et al.*, 2002).

Both myristoylation and palmitoylation increase the hydrophobicity of a protein, favouring membrane association and interaction with hydrophobic protein domains (Benetka *et al.*, 2008). For Ca^{2+} sensors, the localisation at membranes is particularly important as Ca^{2+} signals generally arise at these sites (Das and Pandey, 2010). However, it is unclear how CDPKs are targeted to a specific membrane such as the plasma membrane or the ER despite their apparently identical modifications. A possible explanation for this effect is the 'kinetic trapping' mechanism (Resh, 2006). In this model, a protein that harbours its myristoylation but has not yet been palmitoylated, associates to membranes with a high dissociation rate since myristoylation alone is not sufficient for stable membrane anchoring (Resh, 2006). If this protein is specifically palmitoylated by a PAT residing in the plasma membrane, the protein becomes kinetically trapped at this membrane. Hence, the localisation of the PAT might allow the specific association to membranes (Resh, 2006).

1.7 Specificity of CDPKs

Due to the high number and homologies of CDPK isoforms, it is likely that CDPKs have redundant functions. For instance, whereas single knockout (ko) or knockdown of AtCPK4, AtCPK5, AtCPK6 and AtCPK11 does not alter the susceptibility to pathogens, the quadruple mutant shows severely compromised pathogen defence (Boudsocp *et al.*, 2010). Nevertheless, there are also cases in which a single ko already displays a phenotype, e.g. increased salt-sensitivity has been observed in an *Arabidopsis cpk3* ko line (Mehlmer *et al.*,

2010). Therefore, the current model proposes that some functions of CDPKs are overlapping, but that others are attributed to individual CDPKs. This specificity is established by means of several mechanisms, which are outlined in the next sections.

Expression levels: Some CDPK isoforms exhibit different expression patterns in response to certain stimuli (Ludwig *et al.*, 2004). For instance, several stimuli such as abscisic acid (ABA), gibberellic acid (GA) or wounding induce the expression of NtCDPK1 (Yoon *et al.*, 1999). Moreover, expression of AtCPK10 and AtCPK11 is stimulated by drought or salt stess, but not by heat or cold (Urao *et al.*, 1994). As the induction of a CDPK leads to a greater abundance of these isoforms in response to a stimulus, this mechanism provides a first level of specificity.

Subcellular localisation: Subcellular targeting determines not only which targets a kinase is able to encounter but also which Ca^{2+} signals are primarily sensed. This is important since different stimuli evoke Ca^{2+}spiking at distinct subcellular compartments (Sanders *et al.*, 1999).

Activation by different Ca^{2+} signals: CDPKs might be activated by different levels of Ca^{2+}. In soybean, CDPKα and CDPKγ are activated by Ca^{2+} signals that differ more than tenfold in their magnitude (Harper *et al.*, 2004). In addition, both AtCPK13 and AtCPK23 display an activity of about 50% to 60% in the absence of Ca^{2+} (Kanchiswamy *et al.*, 2010; Geiger *et al.*, 2010). Interestingly, these CDPKs have only two (AtCPK13) or three (AtCPK23) EF hands instead of four, respectively (Cheng *et al.*, 2002). Therefore, it would be worth investigating whether the other *Arabidopsis* CDPKs with less than four EF hands also exhibit unusual Ca^{2+} activation properties.

Substrate specificity: At least some CDPKs display specific recognition of substrates. In *in-vitro* kinase assays, AtCPK3, AtCPK4, AtCPK5 and AtCPK6 show distinguishable phosphorylation patterns of microsomal membranes (Mehlmer, 2008). Since in these assays all the specificity-attributing mechanisms described above are invalidated, this result indicates that CDPKs have an intrinsic substrate specificity. Most likely, this specificity is encoded in the N-terminal domains, which vary considerably both in length and sequence (Cheng *et al.*, 2002). In this respect, Ito and co-workers have recently shown that the transfer of the N-terminal domain from NtCDPK1 to AtCPK9 also relays substrate specificity, demonstrating the importance of the N-terminal variable domain for the recognition of substrates (Ito *et al.*, 2010).

1.8 Functions and Targets of CDPKs

The functional analysis and identification of targets of CDPKs is a challenging issue. Yeast two-hybrid screens, which represent an effective means for identifying interaction partners, have been successfully applied to the cytosolic CDPK AtCPK11 (Rodriguez Milla *et al.*, 2006). In case of membrane-associated CDPKs or targets, however, this approach is likely to fail, as a translocation of the interacting components into the nucleus is required. Furthermore, knockout (ko) lines, which might give important insights into the function of a protein, are not available for all CDPKs (e.g. no T-DNA insertion line for AtCPK4) or may display no phenotypes due to the possible functional redundancy of CDPKs. Therefore, lines with multiple knockouts or lines that overexpress a CDPK are often necessary to observe a phenotype (e.g. Boudsocq *et al.*, 2010; Xu *et al.*, 2010). Another possibility is to transiently inhibit a CDPK prior to stress exposure (Böhmer and Romeis, 2007). Thereby, the plant has less time to compensate the lack of a protein by upregulating or downregulating other proteins in order to suppress a phenotype (Böhmer and Romeis, 2007). However, inhibitors specific for individual CDPKs are not available (Cheng *et al.*, 2002). To circumvent this problem, Böhmer and Romeis have created an ATP-analogue-sensitive (as) kinase variant (Liu *et al.*, 1998) of AtCPK1 that is specifically inhibited by the chemical compound 1-NA-PP1 (Böhmer and Romeis, 2007). This as-AtCPK1 was expressed in the *cpk1* ko background to simulate a wild-type plant in case of the absence of 1-NA-PP1. By adding 1-NA-PP1 to these *as-AtCPK1* plants shortly before exposure to cold, as-AtCPK1 was specifically inhibited mimicking a transient *cpk1* ko plant. Thereby, several differences in phosphorylation patterns between the *as-AtCPK1* and the wild-type line upon cold stress have been observed (Böhmer and Romeis, 2007). However, it has not been demonstrated that these changes are not observed in the *Atcpk1* ko, rendering unclear whether this approach is worth the effort.

In addition to AtCPK1, several other CDPKs regulate abiotic stress responses. For instance, ko plants of AtCPK10 and AtCPK8 display a drought-sensitive phenotype (Wu *et al.*, 2010). Similarly, *Arabidopsis cpk3* ko lines have recently been demonstrated to show impaired salt-stress acclimation (Mehlmer *et al.*, 2010). Moreover, whereas no phenotype has been observed in an *Arabidopsis cpk6* ko line under drought/salt stress, overexpression of AtCPK6 conferred higher tolerance under these conditions (Xu *et al.*, 2010). Similarly, overexpression of rice OsCDPK7 resulted in increased tolerance to cold and drought/salt stresses (Saijo *et al.*, 2000). Although these examples demonstrate the importance of CDPKs

in abiotic stress responses, it should be noted that no direct targets of CDPKs have been identified in this respect so far.

CDPKs are also components of response to biotic stresses. Using virus-induced gene silencing (VIGS) of NtCDPK2 and NtCDPK3, Romeis and co-workers have shown that these two CDPKs are positive regulators of the hyper-sensitive response (HR) in tobacco upon race-specific elicitation (Romeis *et al.*, 2001). In *Arabidopsis*, the quadruple knockout/knockdown of AtCPK4, 5, 6 and 11 displayed reduced oxidative burst and elevated growth of pathogens, demonstrating the important role of these CDPKs in innate immunity (Boudsocq *et al.*, 2010). AtCPK1 may have a function in the regulation of oxidative burst as well, as this CDPK significantly increased the activity of the NADPH oxidase in tomato protoplasts (Xing *et al.*, 2001). Interestingly, a potato homologue of NADPH oxidase has been conclusively shown to be regulated by StCDPK5 *in vivo*, representing one of the first *bona fide* targets of which the corresponding CDPK has been identified so far (Kobayashi *et al.*, 2007).

Another function of CDPKs is the regulation of phytohormone signalling. NtCDPK1 has been identified as a kinase and negative regulator of the transcription factor RSG (REPRESSION OF SHOOT GROWTH), which enhances the transcription of an enzyme involved in the gibberellic acid biosynthesis (Ishida *et al.*, 2008). In ABA-mediated signalling, AtCPK32 phosphorylates and thereby activates the ABA-responsive bZIP transcription factor ABF4 (Choi *et al.*, 2005). In addition, Zhu *et al.* (2007) have reported that *Arabidopis cpk4 cpk11* double ko plants exhibit an ABA-insensitive phenotype such as an increased germination under ABA treatment. However, these results have to be handled carefully since the used *cpk4* ko line appeared to be no complete knockout in our hands.

ABA-mediated signalling is also essential in stomatal closure. In this respect, the double ko of AtCPK3 and AtCPK6 displays decreased Ca^{2+}- and ABA-dependent activation of guard cells S-type anion channels, resulting in a significantly impaired ABA-regulated stomatal closure (Mori *et al.*, 2006). Moreover, AtCPK21 and AtCPK23 phosphorylate and thereby activate the guard cell anion channel SLAC1 (SLOW ANION CHANNEL-ASSOCIATED 1) in an ABA-sensitive manner (Geiger *et al.*, 2010). Involvement of CDPKs in the stomatal movement has also been proposed in soybean, where a CDPK phosphorylates the guard cell K^+ channel KAT1 *in vitro* (Li *et al.*, 1998).

CDPKs have been implicated in carbon and nitrogen metabolism as well, in particular by regulating the activity of sucrose synthase (SuSy), sucrose-phosphate synthase (SPS), and nitrate reductase (NR) (Cheng *et al.*, 2002). This is interesting, as energy metabolism is

closely linked to stress responses (Baena-Gonzalez and Sheen, 2008). SuSy catalyses the reversible conversion of sucrose and UDP to glucose-UDP and fructose (Hardin *et al.*, 2004), and has been shown to be phosphorylated by CDPKs at a conserved Ser close to the N terminus (Cheng *et al.*, 2002). In maize, this phosphorylation influences the membrane association of SuSy (Hardin *et al.*, 2004) and enhances its affinity for sucrose and UDP in a pH-dependent manner, favouring the cleavage of sucrose (Huber *et al.*, 1996). In contrast, phosphorylation of SPS and NR, two key enzymes in sucrose synthesis and nitrogen assimilation, respectively, is part of their dark inactivation (McMichael *et al.*, 1995; Cheng *et al.*, 2002). Isolation of their corresponding kinases by chromatography from spinach leaves has revealed three kinase peaks: Peak I activity inhibited both SPS and NR, whereas peak II and III activities specifically inhibited NR or SPS, respectively (McMichael *et al.*, 1995). Peak I later turned out to contain a CDPK and peak III containes the SNF1-related protein kinase SnRK1, both of which phosphorylate Ser158 of SPS *in vitro* (Cheng *et al.*, 2002). Similarly, the NR inhibiting kinase activity of peak I was identified as a CDPK that displays high similarity to AtCPK3 (Douglas *et al.*, 1998). However, phosphorylation of Ser543 of NR in the dark is not sufficient for inactivation but allows the binding of a 14-3-3 protein to the phosphorylated Ser543, which then inhibits NR (Cheng *et al.*, 2002). Interestingly, kinase activity of peak II has also results from a CDPK (Cheng *et al.*, 2002), demonstrating the extensive role of CDPKs in regulating these enzymes involved in carbon and nitrogen metabolism (Cheng *et al.*, 2002).

1.9 AtCPK3

AtCPK3 (At4g23650; called CPK3 in this manuscript) is a 59 kDa protein kinase that belongs to the subgroup II of *Arabidopsis* CDPKs (Fig. 1.4.1; Cheng *et al.*, 2002). Besides its role in ABA-mediated stomatal closure (Mori *et al.*, 2006), CPK3 has recently been shown to be involved in biotic as well as abiotic stress responses (Kanchiswamy *et al.*, 2010; Mehlmer *et al.*, 2010). First, a role in the defence response against the caterpillar *Spodoptera littoralis* has been reported for both CPK3 and CPK13 (Kanchiswamy *et al.*, 2010). In this study, a *cpk3* ko line did not display any obvious phenotype, but a decreased induction of the plant defensin gene *PDF1.2* upon caterpillar attack was observed. Interestingly, using a set of 100 *in-vitro* translated substrates, the heat-shock factor HsfB2a has been identified to be phosphorylated *in vitro* by both CDPKs and to enhance transcription of *PDF1.2* in a CPK3-dependent manner in tobacco leaves (Kanchiswamy *et al.*, 2010). Second, it has been

reported that the expression of CPK3 in transgenic *cpk3* ko and overexpressing lines positively correlates with tolerance towards salt stress, demonstrating its important role in salt-stress acclimation (Mehlmer *et al.*, 2010). Surprisingly, induction of several stress-related genes appeared to be normal in these lines. Therefore, it was suggested that CPK3 might be involved in the rapid phosphorylation of ion channels or transporters rather than in the transcriptional reprogramming in response to salt-stress (Mehlmer *et al.*, 2010).

Although no targets of CPK3 have been presented in this report, a proteomics approach using phosphorylation of roots microsomes by CPK3, 2D-gel separation, and mass-spectrometry based protein identification revealed several putative CPK3 targets (Table 1; Mehlmer *et al.*, 2010). These included (i) the glutathione-*S*-transferase ERD13 (Edwards *et al.*, 2000); (ii) a remorin protein (Rafaele *et al.*, 2007); (iii) KAB1, which is a regulating subunit of K^+ channels (Tang *et al.*, 1996; Zhang *et al.*; 1999); (iv) a protein of unknown function; (v) calreticulins 1 and 2, which are involved in Ca^{2+} binding (Jia *et al.*, 2009); and (vi) a phosphatase belonging to the PP2C family (Schweighofer *et al.*, 2004). Importantly, several of these candidates are implicated in salt-stress signalling (Mehlmer *et al.*, 2010). Therefore, this list provides interesting putative targets of CPK3 that are worth being investigated further.

	AGI	Annotation	*P*-score
→	AT2G30870	**ERD13, glutathione-*S*-transferase PHI 10**	32
→	AT2G45820*	**Remorin, putative DNA-binding protein, salt-induced**	22
→	AT1G04690	**KAB1, KV-BETA1 (potassium channel beta subunit)**	18
→	AT3G18240*	**Unknown protein, phosphorylated**	18
	AT1G53070*	**Legume lectin family protein, cell wall asscociated**	15
→	AT1G09210*	**CRT2, Calreticulin 2; calcium ion binding**	13
→	AT1G56340*	**CRT1, Calreticulin 1; calcium ion binding**	12
	AT5G38480*	**GRF3, 14-3-3 PSI, overexpression confers salt tolerance**	9
→	AT3G02750*	**PP2C, protein phosphatase 2C family, group E**	9
	AT5G19440	**CAD, Cinnamyl-alcohol dehydrogenase, putative**	9
	AT3G18820	**RAB71, (Arabidopsis RAB GTPase homolog G3F); GTP binding**	8
	AT2G02990	**RNS1, (Ribonuclease 1); cell wall/plasma membrane associated**	8

Table 1. Excerpt of putative targets of CPK3 identified via 2D-phosphoproteomics. The P-score indicates the over-representation of consensus CDPK phosphorylation sites in the protein compared to the Arabidopsis genome. Asterisks refer to proteins of which phosphorylated peptides are listed in the Phosphat 3.0 database. Proteins used in the present study are indicated with arrows (modified from Mehlmer *et al.*, 2010).

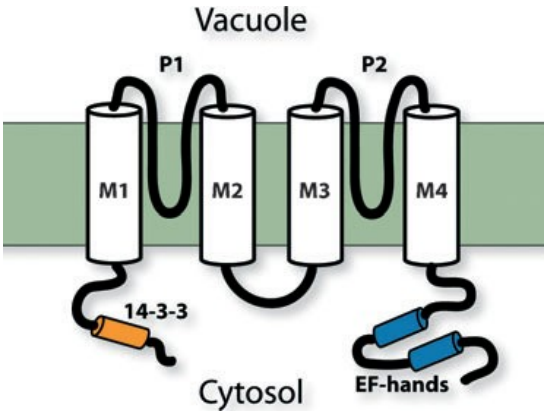

Figure 1.9.1. Topology of TPK1. The four transmembrane domains (M1-4) are shown as white barrels. P1 and P2 refer to the two pore regions. 14-3-3, 14-3-3 binding motif (Latz *et al.*, 2007).

Another possible target of CPK3 is two-pore K^+ channel 1 (TPK1). This is a presumably dimeric voltage-independent K+ channel that is located in the vacuolar membrane and harbours interesting structural features (Fig. 1.9.1; Latz *et al.*, 2007). At its cytosolic C-terminal domain, TPK1 has two Ca^{2+} binding EF hands that lead to closure of the channel in the absence of Ca^{2+} (Latz *et al.*, 2007). Moreover, it contains a 14-3-3 site at its N-terminal cytosolic domain. Preferentially upon phosphorylation of this site, the 14-3-3 protein GRF6 binds to it and thereby increases the activity of TPK1 (Latz *et al.*, 2007). However, the corresponding kinase has not been identified so far. Kinase assays using soluble and microsomal protein extracts and the N-terminal domain of TPK1 as substrate revealed that TPK1 is phosphorylated by a soluble kinase activity in a Ca^{2+} dependent manner (Latz *et al.*, unpublished). This result strongly suggests that a cytosolic CDPK such as CPK3 is capable of phosphorylating TPK1.

1.10 Aim of This Work

The aim of this work was to analyse the subcellular localisation of CPK3 in order to gain insights into the functions of this kinase in response stress. In particular, I was interested in the membrane association of CPK3. Using highly pure plasma membrane that was isolated via two-phase partitioning, I show that CPK3 is associated with the plasma membrane. Furthermore, I separated membranes according to their density in sucrose density gradients. This experiment revealed that CPK3 is associated with the vacuolar membrane in leaves, but not in roots, suggesting different functions of CPK3 in these two organs.

As a second project, I analysed the interaction between CPK3 and putative targets of CPK3 (described above, Table 1). Using bimolecular fluorescence complementation (BiFC), I was

able to show that CPK3 interacts with ERD13, remorin, the protein of unknown function and PP2C-type phosphatases *in planta*. This result provides a first evidence for the involvement of CPK3 in the regulation of these proteins. Moreover, BiFC studies revealed that TPK1 and CPK3 interact *in vivo* as well. Importantly, this interaction was significantly reduced when two arginines in the predicted interaction domain of TPK1 were mutated to alanine, demonstrating the specificity of this interaction.

2 Materials and Methods

2.1 Buffers, Solutions and Media

13.5-g phase system: 6.4% (w/w) Dextran T-500, 6.4% (w/w) PEG 3,350, 5 mM potassium phosphate buffer pH 7.8, 5 mM KCl, 300 mM sucrose, altogether 13.5 g

Acrylamide: 30% 37.5:1 acrylamide:bisacrylamide (Bio-Rad)

Anode buffer I: 300 mM Tris-HCl pH 10.4, 10% methanol

Anode buffer II: 25 mM Tris-HCl pH 10.4; 10% methanol

Bradford reagens: 20% Protein Assay (Bio-Rad)

Cathode buffer: 25 mM Tris-HCl pH 9.4, 40 mM glycine, 10% methanol

Coomassie staining solution: 0.25% coomassie brilliant blue R-250, 10% isopropanol, 10% acetic acid

Centrifugation buffer 20% sucrose with EDTA: 10 mM Tris-HCl pH 7.5, 5 mM EDTA, 20% (w/w) sucrose

Centrifugation buffer 50% sucrose with EDTA: 10 mM Tris-HCl pH 7.5, 5 mM EDTA, 50% (w/w) sucrose

Centrifugation buffer 20% sucrose with Mg^{2+}: 10 mM Tris-HCl pH 7.5, 2 mM EDTA, 15 mM $MgCl_2$, 20% (w/w) sucrose

Centrifugation buffer 50% sucrose with Mg^{2+}: 10 mM Tris-HCl pH 7.5, 2 mM EDTA, 15 mM $MgCl_2$, 50% (w/w) sucrose

Enzyme lysis buffer: 25 mM Tris-HCl pH 7.5, 20 mM NaCl, 8 mM $MgCl_2$, 5 mM DTT, 0.1% NP-40

Ethidium bromide solution: 5 mg/ml ethidium bromide

Destaining solution: 10% isopropanol, 10% acetic acid

Basal mineral medium: 2.5 mM $NaNO_3$, 2.5 mM $Ca(NO_3)_2$, 2 mM $MgSO_4$, 2 mM $NH_4H_2PO_4$, 0.1 mM NaFeEDTA, 25 µM $CaCl_2$, 25 µM H_3BO_3, 2 µM $ZnSO_4$, 2 µM $MnSO_4$, 0.5 µM $CuSO_4$, 0.2 µM Na_2MoO_4, 2.5 mM MES, pH 5.7 with NaOH (~ 1 mM NaOH), 0.7% agarose

Hoagland medium: 5 mM $Ca(NO_3)_2$, 1 mM KH_2PO_4, 5 mM KNO_3, 2 mM $MgSO_4$, 2 mg/l Fe-EDTA, 46 µM H_3BO_3, 11 µM $MnCl_2$, 0.8 µM $ZnSO_4$, 0.3 µM $CuSO_4$, 0.1 µM MoO_3

Homogenisation buffer with EDTA: 400 mM sorbitol, 50 mM Tris-HCl pH 7.8, 10 mM EDTA, 1 mM DTT, 1 complete tablet EDTA-free (Roche) per 100 ml

Homogenisation buffer with Mg^{2+}: 400 mM sorbitol, 50 mM Tris-HCl pH 7.8, 2 mM EDTA, 15 mM $MgCl_2$, 1 mM DTT, 1 complete tablet EDTA-free (Roche) per 100 ml

Homogenisation buffer for TPP: 50 mM Tris pH 8.0 adjusted with MES, 400 mM sorbitol, 20 mM EDTA, 20 mM EGTA, 50 mM NaF, 15 mM β-glycerophosphate, 1 mM Na-orthovanadate, 10 mM ascorbic acid, 5 mM DTT, 1 complete tablet EDTA-free (Roche) per 100 ml

LB (lysogeny broth) medium: 1% peptone, 0.5% yeast extract, 0.5% NaCl, supplemented with 2% agar (in case of plates) and antibiotics (50 mgl/l kanamycin or 100 mg/l ampicillin), if required

Microsome resuspension buffer with EDTA: 10 mM Tris-HCl pH 7.5, 5 mM EDTA, 55% (w/w) sucrose

Microsome resuspension buffer with Mg^{2+}: 10 mM Tris-HCl pH 7.5, 2 mM EDTA, 15 mM $MgCl_2$, 55% (w/w) sucrose

Microsome resuspension buffer for TPP: 5 mM potassium phosphate buffer pH 7.8, 330 mM sucrose, 2 mM DTT, 10 mM NaF

½-MS medium: 0.22% Murashige & Skoog medium incl. Gamborg B5 vitamins (Duchefa Biochemie), 0.7% plant agar (Duchefa Biochemie), pH 6.0 with 0.1 M KOH

ONPG solution: 4 mg/ml ONPG (ortho-Nitrophenyl-β-galactoside)

P1: 50 mM Tris-HCl pH 8.0, 10 mM Na_2EDTA, 100 µg/ml RNase

P2: 200 mM NaOH, 1% SDS

P3: 3 M potassium acetate, pH 5.5

PM preserving buffer: PM membrane washing buffer made up with 5 mM DTT and one complete tablet EDTA-free (Roche) per 100 ml

PM washing buffer: 10 mM Tris base, 10 mM boric acid, 300 mM sucrose, 9 mM KCl, 5 mM EDTA, 5 mM EGTA, 50 mM NaF, pH 8.3 with MES or Tris base

2x Separating gel buffer: 1.5 M Tris-HCl pH 8.8, 0.1% SDS

SD-leu-trp medium: 0.46% YNB (yeast nitrogen base), 2% glucose, 30 mg/l arginine, 20 mg/l histidine, 20 mg/l isoleucine, 20 mg/l methionine, 40 mg/l lysine, 40 mg/l tyrosine, 40 mg/l uracil, 40 mg/l adenine, 60 mg/l phenylalanine, 65 mg/l valine, 100 mg/l aspartate, 3% agar (in case of plates)

2x SDS sample buffer: 50% glycerol, 2% SDS, 5% β-mercaptoethanol, 125 mM Tris-HCl pH 6.8

SDS running buffer: 0.1% SDS, 25 mM Tris base, 250 mM glycine

2x Stacking gel buffer: 0.25 M Tris-HCl pH 6.8, 0.1% SDS

1x TAE: 40 mM Tris acetate, 1 mM Na_2EDTA, pH 8.0

TBS-T: 50 mM Tris-HCl pH 7.4, 150 mM NaCl, 0.05-0.1% Tween-20

Transformation buffer: 10 mM $CaCl_2$, 10 mM Pipes-NaOH, 15 mM KCl_2, 55 mM $MnCl_2$, pH 6.7

Transformation mix: 800 µl 50% PEG 4,000, 100 µl of 2 M lithium acetate, 100 µl of 1 M DTT, 20 µl of bacterial RNA (10 µg/µl)

YPD: 2% peptone, 1% yeast extract, 2% glucose, 3% agar (in case of plates)

Z buffer: 60 mM Na_2HPO_4, 40 mM NaH_2PO_4, 10 mM KCl, 1 mM $MgSO_4$, 0.5% β-mercaptoethanol

2.2 DNA Methods

2.2.1 Agarose Gel Electrophoresis

According to the size of the DNA fragment, 0.7-1.5% agarose gels were prepared in 1x TAE buffer with 5 µl of ethidium bromide solution per 100 ml of agarose gel. 1x TAE was used as running buffer. DNA loading buffer was added to the DNA samples, and the GeneRuler™ 1kb DNA Ladder Plus (Fermentas) was used as marker. Gels were run at 90-150 kV for 30-60 min. The DNA was visualised under UV light.

2.2.2 Purification of DNA

To elute DNA fragments from an agarose gel or to purify DNA, the Wizard® SV Gel and PCR Clean-Up System (Promega) was used according to the manufacturer's protocol. The DNA was eluted in 40 µl of nuclease-free water.

2.2.3 Determination of DNA Concentration

Concentration of DNA was determined using NanoDrop® UV-Vis spectrophotometer (PEQLAB) according to the manufacturer's instructions.

2.2.4 Preparation of Plasmid DNA from *E. coli* (Quick-Prep)

2 ml of an *E. coli* overnight culture were transferred to an Eppendorf tube and centrifuged at 16,100 x *g* for 1 min at room temperature. After removal of the supernatant, the cells were resuspended in 200 µl of buffer P1. Then 200 µl of buffer P2 were added, and the solution was mixed by inverting the tube for few times. 200 µl of buffer P3 was added and mixed similarly. The tubes were cooled on ice and centrifuged at 16,100 x *g* for 15 min at 4°C. The supernatant was carefully transferred to a fresh tube, and the DNA was precipitated by adding 70% of the volume's isopropanol. The solution was mixed thoroughly and cooled on

ice for two minutes. DNA was recovered by centrifuging at 16,100 x *g* for 15 min at 4°C. The supernatant was removed, and the pellet was rinsed with 200 µl of 70% ethanol for 5 min. The ethanol was removed carefully with a pipette. The pellet was dried for 15 min at 40°C and the plasmid DNA was resolved in 50 µl of nuclease free water.

To increase the yield in case of low-copy plasmids (pBIN19, pSCYNE, and pSCYNE(R) vectors), the protocol described above was slightly modified: 4 ml of the overnight culture and 300 µl of the buffers P1, P2 and P3 were used. At the end, the pellet containing the plasmid DNA was resolved in only 35 µl of water.

2.2.5 Analytical Digestion of Plasmids

To determine whether the plasmids obtained by quick-prep (2.2.4) are correct, digestions with restriction enzymes were performed. Therefore, 3-5 µl of plasmid DNA (8 µl in case of pBIN vectors) were mixed with 0.2-0.5 µl of restriction enzymes (NEB) in a total volume of 20 µl according to the manufacturer's instructions. The digests were incubated for 1.5 h hours at the recommended temperature. The obtained fragments were analysed by agarose gel electrophoresis.

2.2.6 Preparative Digestion of Plasmids

For cloning purposes, 5 µg of plasmid DNA were digested for 2 h in a total volume of 40 µl with 0.3-0.6 µl of restriction enzymes (NEB) according to the manufacturer's instructions. The DNA fragments were separated by agarose gel electrophoresis (2.2.1), cut out with a scalpel and purified as described (see 2.2.5).

2.2.7 Ligation of DNA

Ligations were performed in 10 µl reactions using purified DNA fragments and 0.5 µl of T4 ligase (NEB). Insert was added in 4 times excess in molar concentrations compared to the vector backbone. The reactions were incubated at room temperature for 20 min prior to transformation into *E. coli* (2.4.3).

2.2.8 Polymerase Chain Reaction (PCR)

Cloning of constructs: For cloning of constructs out of a cDNA library, PCR was performed with the Phusion™ High-Fidelity DNA Polymerase (Finnzymes). A 50 µl reaction usually contained 5 µl of 5x buffer (Finnzymes), 1 µl of dNTPs (10 mM each,

NEB), 2.5 µl of each primer (10 µM) and 100 ng of an *Arabidopsis* cDNA library (kindly obtained from François Lacroute and Simon Stael). The PCR program is described below. The PCR fragments were cloned into pCR-Blunt from the Zero Blunt® PCR Cloning Kit (Invitrogen) according to the manufacturer's protocol and analysed by sequencing (Microsynth AG or Agowa) prior to subcloning.

Site-directed mutagenesis: Site-directed mutagenesis was performed with the Phusion™ High-Fidelity DNA Polymerase (Finnzymes). The reaction had the same composition as described above, but instead of the cDNA library, 10 ng of *TPK1* in pBAT was used as template. The PCR program is described below. To get rid of the original template plasmid, the PCR product was digested with *Dpn*I (NEB), according to the manufacturer's protocol. Afterwards, it was purified with agarose gel electrophoresis (see 2.2.1), eluted from the gel (see 2.2.2), re-ligated (see 2.2.7) and transformed into *E. coli* (see 2.4.3). After isolation of the plasmids, the introduction of the mutation was confirmed via sequencing.

Colony-PCR of *Agrobacteria*: Colony-PCR with GoTaq polymerase (Promega) was performed to confirm the presence of a plasmid in *Agrobacteria*. A typical 25 µl reaction contained 0.125 µl of dNTPs (10 mM each, NEB), 5 µl of buffer (Promega), 0.125 µl of polymerase and 1 µl of each primer (10 µM). *Agrobacterium* cells were added by picking visible amounts of a colony from a plate with a tip and dipping this tip several times vehemently into the PCR mix. The tips were furthermore used to inoculate cultures. For each primer pair a complete PCR reaction was prepared containing non-corresponding *Agrobacteria*. The PCR program is described below.

PCR programs:

For cloning	For mutagenesis:	For colony-PCR:
98°C 30 s	98°C 2 min	95°C 5 min 1x
~54°C 30 s 1x	61°C 2 min 1x	----------
72°C 2 min	72°C 10 min	95°C 45 s
----------	----------	52°C 45 s 30x
98°C 15 s	98°C 45 s	72°C 90 s
~54°C 30 s 35x	61°C 2 min 30x	----------
72°C 15-30 s / kb	72°C 10 min	72°C 5 min 1x
----------	----------	
72°C 10 min 1x	72°C 15 min 1x	

2.2.9 Primers

For cloning, primers were designed that span the whole coding sequence (CDS) except for the stop codon. To allow the subcloning into compatible vectors, an *Apa*I site in front of the start codon was introduced into the construct, and the stop codon was replaced by a *Not*I site. In case of site-directed mutagenesis of *TPK1*, the mutation was introduced approximately in the middle of the forward primer together with a new *Bss*HII restriction site close to the mutation. The reverse primer was designed in a way that it binds to the template exactly adjacent to the 5'end of the forward primer without any overlaps. To increase the efficiency of the re-ligation of the PCR product prior to transformation into *E. coli*, the forward primer was ordered with phosphorylation of its 5' end. In addition, the primers were ordered as purified via PAGE (forward primer) or HPLC (reverse primer). Sequences of primers are listed in table 2. All primers were produced by Microsynth AG.

2.2.10 Vectors

pACTIIJ: Yeast two-hybrid vector carrying the Gal4 transcriptional activator domain

pBAT: Relatively small *in-vitro* transcription and translation vector which was used to introduce point mutations into *TPK1*

pSCYNE and pSCYNE (R): Binary vector obtained from Jörg Kudla (Waadt *et al.*, 2008) modified by Andrea Mair for *Apa*I/*Not*I cloning system. These vectors were used for transient expression of proteins in BiFC assays. Proteins are either fused to the C-terminal half of CFP (ctCFP) together with a HA-tag or fused to the N-terminal half of CFP (ntCFP) with a FLAG-tag.

pBIN19: Binary vector used for transient expression of proteins in tobacco leaves. Protein are either N- or C-terminally fused to mCherry or C-terminally to YFP.

pBTM117: Yeast two-hybrid vector carrying the LexA DNA-binding domain

Primers for cloning and point mutagenesis		
Name	*Sequence*	*ID (TAIR)*
ERD13 fw	5'-GGGCCCATGGTGTTGACAATCTATGC-3'	AT2G30870
ERD13 rev	5'-GCGGCCGCAAACAGGTAGTGAG-3'	
Kab1 fw	5'-GGGCCCATGCAGTACAAGAATCTGG-3'	AT2G45820
Kab1 rev	5'-AAAGCGGCCGCACCTATATGATTCAGG-3'	
PP2C fw	5'-GGGCCCATGGGGTCCTGTTTATCTGC-3'	AT3G02750
PP2C rev	5'-GCGGCCGCACTTTCCAGGCA-3'	
REMO fw	5'-GGGCCCATGGCGGAGGAGCAAAAGACG-3'	AT2G45820
REMO rev	5'-GCGGCCGCAGAAACATCCACACG-3'	
unknown protein fw	5'-TAAGGGCCCATGAGAGGAGCTCTC-3'	AT3G18240
unknown protein rev	5'-GCAAGCGGCCGCAAGCGTTGATGGC-3'	
CRT1 sf1 fw	5'-AAAGGGCCCATGGCGAAACTAAACCC-3'	AT1G56340
CRT1 sf1 rev	5'-TAAGCGGCCGCAGAGCTCGTCATGGG-3'	
CRT2 fw	5'-TAAAGGGCCCATGGCGAAAATGATTCC-3'	AT1G09210
CRT2 rev	5'-AATAGCGGCCGCATAGCTCATCATGAGC-3'	
SOS1 fw	5'-AAAGGGCCCATGACGACTGTAATCG-3'	AT2G01980
SOS1 rev	5'-TTTGCGGCCGCATAGATCGTTCC-3'	
GAPC fw	5'-AAAGGGCCCATGGCTGACAAGAAG-3'	AT3G04120
GAPC rev	5'-TTTGCGGCCGCAGGCCTTTGACATG-3'	
NHX1 fw	5'-AAAGGGCCCATGTTGGATTCTC-3'	AT5G27150
NHX1 rev	5'-TGCGGCCGCTAGCCTTACTAAGATCAGGAGG G-3'	
AP2C fw	5'-AAAGGGCCCATGTCTTGCTCCGTCGC-3'	AT2G30020
AP2C rev	5'-AAAGCGGCCGCATATGAACTGGCGTAAAGG-3'	
TPK1 R35R39-A fw	5'CTTCAAGAAAAGCAAGATTGCGCGCGGTCTAGA AGTGCTCC-3'	AT5G55630
TPK1 R35R39-A rev	5'-AAGAAGTTCTTGAGTTCAGG-3'	

Primers for sequencing		
Name	*Sequence*	*ID (TAIR)*
Seq1SOS1 fw	5'-CCCTGATGAATGATGGGACG-3'	AT2G01980
Seq2SOS1 fw	5'-TTGTTCTACGCCTTCTTCGC-3'	
Seq3SOS1 fw	5'-CCGATCTTCATTTCCTCAGG-3'	

Table 2. Primers used for cloning, site-directed mutagenesis and sequencing of constructs.

2.3 Protein Methods

2.3.1 SDS-Polyacrylamid Gel Electrophoresis (SDS-PAGE)

Protein samples were prepared by adding SDS-sample buffer, boiling at 95°C for 5 min, cooling on ice and short centrifugation. In case of primarily hydrophobic proteins, the samples were not boiled. The gel chamber MiniProtean® 3 (Bio-Rad) was assembled according to the manufacturer's instructions and filled with SDS running buffer. 4 µl of

PageRuler™ Plus Prestained Protein Ladder from Fermentas were loaded as marker. Gels (see table 3) were run with 20 mA per gel until the colour front had passed the stacking gel and were then set to 40 mA per gel.

	Mini-gels (0.75 mm) (for 4 gels)		
	12% separating gel	*8% separating gel*	*4% stacking gel*
30% acrylamide	6 ml	4 ml	0.8 ml
ddH_2O	1.36 ml	3.36	2.15 ml
2x buffer	7.5 ml	7.5 ml	3 ml
TEMED	30 µl	30 µl	12 µl
10% APS	110 µl	110 µl	42 µl
Total	15 ml	15 ml	6 ml

Table 3. Composition of four 12% or 8% SDS-PAGE gels, respectively.

2.3.2 Coomassie Staining

SDS-PAGE gels were stained in coomassie staining solution by brief heating in the microwave and shaking for 10 min at room temperature. In case of membranes, the coomassie was not heated. For destaining, the staining solution was replaced by destaining solution. Again, the solution was boiled shortly (also for membranes) and incubated for 10 minutes at room temperature. Fresh destaining solution was added several times until the gel or membrane was completely destained. Gels were dried in a gel dryer for 1.5 h at 70°C. Membranes were dried on a tissue paper or Whatman paper on the bench.

2.3.3 Western Blot

Proteins were transferred to PVDF membranes (Hybond™-P from GE Healthcare or Immobilon TM-P transfer membrane from Millipore) using the Trans-Blot® Semi-Dry blotting chamber from Bio-Rad. After separation of proteins by SDS-PAGE, the stacking gel was removed and the separating gel incubated in cathode buffer for 15 min under gentle shaking. The membrane was placed in methanol for 10 seconds, then incubated in water for 5 minutes under shaking and afterwards equilibrated in anode buffer II for another 5 minutes. For assembling of the Western blot, one thin Whatman paper with the size of the gel was soaked in anode buffer I and laid onto the blotting chamber, followed by two other Whatman papers soaked with anode buffer II. The membrane was placed onto the papers, and the gel was laid onto the membrane. The stack was completed with three Whatman papers soaked with cathode buffer. To remove air bubbles within the stack, an even tube was

carefully rolled over the stack. The blotting chamber was closed and the transfer was done at 80 mA per gel and 16 V for one hour.

Afterwards, the membrane was incubated in blocking solution (either 5% skimmed milk powder solution in TBS-T or 1% BSA in TBS-T) for one hour at room temperature under gentle shaking. Then the membrane was incubated in blocking solution completed with the primary antibody overnight at 4°C or for 1-2 hours at room temperature on a shaker. The membrane was washed three times with TBS-T for 5 min each. Subsequently, the membrane was incubated with the HRP-conjugated secondary antibody in blocking solution for one hour at room temperature under shaking. Again, the membrane was washed three times with TBS-T for 5 min each. Signals were detected using the SuperSignal West Pico Chemiluminescent Substrate from Pierce or the ECL Plus™ Western Blotting Detection Reagents from GE Healthcare according to the manufacturer's instructions.

2.3.4 Antibodies

αCPK3 antibody: specific antibody raised against the C terminus of CPK3 (Mehlmer *et al.*, 2010)

αH$^+$-ATPase antibody: marker for plasma membrane (AS07 260, Agrisera)

αV-ATPase antibody: marker for vacuolar membrane (AS07 213, Agrisera)

αPorin antibody: marker for mitochondrial membrane; kindly provided by Harvey Millar

αSar1 antibody: marker for ER/Golgi (AS08 326, Agrisera)

αHA antibody: for detection of HA-tagged proteins (Roche, 11867423001)

αFLAG antibody: for detection of FLAG-tagged proteins (Sigma, F3165)

αrabbit IgG HRP-conjugated: secondary antibody (GE Healthcare, NA934)

αmouse IgG HRP-conjugated: secondary antibody (GE Healthcare, NA9310)

αrat IgG HRP-conjugated: secondary antibody (GE Healthcare, NA935)

2.3.5 Protein Extraction from Tobacco Leaves (Quick Method)

A small piece of tobacco leaf (~7 x 7 mm) was quick-frozen in liquid nitrogen in a 2 ml Eppendorf tubes containing two glass beads. The material was crushed for 30 s with 30 Hz in the Tissue Lyzer II (Quiagen). Then, 200 µl of SDS-loading buffer were added, and the sample was vortexed for 2 min. The sample was centrifuged for 10 min at 16,100 x *g* at 4°C, and the supernatant was transferred to a fresh tube. Finally, the obtained protein extract was

boiled at 95°C for 5 min, cooled on ice, centrifuged for 1 min at 16,100 x *g* at room temperature and stored at -20°C.

2.3.6 Determination of Protein Concentration (Bradford Assay)

950 µl of Bradford reagent was mixed with 50 µl of protein sample and incubated for 5-15 min at room temperature. The extinction was measured at 595 nm. Yeast protein extracts were measured 1:10 diluted in 50 mM Tris-HCl pH 7.5.

To obtain a BSA standard curve, solutions with BSA concentrations of 0.025, 0.1, 0.2, and 0.3 mg/ml in 50 mM Tris-HCl pH 7.5 were prepared and measured as described above.

2.3.7 Separation of Membranes from *Arabidopsis* Using Density Gradients

The procedure was either done in the presence of free Mg^{2+} (all buffers with excess of Mg^{2+}, "with Mg^{2+}") or in the absence of free Mg^{2+} (all buffers supplied with EDTA, "with EDTA"). All steps were performed at 4°C.

For one gradient, 10-12 g of plant material (leaves or roots) was harvested from 8-weeks-old hydroponically grown plants. The roots were washed with cold distilled water, softly dried in paper towels and cut with scissors prior to homogenisation and weighing. The material was homogenised in 100 ml of homogenisation buffer in a Waring blender four to six times for 3 s at maximum speed. The homogenate was filtered through two layers of miracloth (Calbiochem) and centrifuged at 10,000 x *g* for 20 min in a SW28 rotor (Beckman Coulter). To obtain the microsomal fraction, the supernatant was centrifuged at 100,000 x *g* for 1 h in the same rotor. The microsomal pellet was rinsed with 1 ml of microsome resuspension buffer and transferred to an Eppendorf tube filled with 100 µl of microsome resuspension buffer. Another 100 µl of this buffer were added together with 200 µl of sea sand. The pellet was resuspended with a glass homogeniser attached to a drill force (RW16 basic, IKA Labortechnik) for three times at full speed for one minute, with one minute of cooling in between. Finally, microsome resuspension buffer was added to a total volume of 0.5 ml.

The resuspended microsomes were transferred without any sea sand to the bottom of a 14 ml thinwall polyallomer tube (Beckman Coulter). Then, a linear sucrose gradient of 20-50% was layered over the sample with a gradient maker using 6 ml of each of the two centrifugation buffers with 20 or 50% sucrose. The gradient was centrifuged for 18 h at 100,000 x *g* in a SW40Ti rotor (Beckman Coulter).

Afterwards, 13 fractions of 1 ml each were carefully taken from the top of the gradient. The sucrose concentration was measured with a refractometer (Pal-1, Atago). 200 µl of the samples were mixed SDS-sample buffer and stored at -20°C. The density gradients were analysed by Western blotting (see 2.3.3) using antibodies for CPK3 and markers for the plasma membrane, the tonoplast, the mitochondrial membrane and the ER/Golgi (see 2.3.4).

2.3.8 Isolation of Plasma Membrane Using Two-Phase Partitioning (TPP)

Plasma membranes were isolated in an aqueous two-phase system according to Mehlmer *et al.* (2010). All steps were done at 4°C. First, the microsomal fraction of 15 g leaves was obtained as described in section 2.3.7 but with the "homogenisation buffer for TPP" as homogenisation buffer. The microsomal pellet was well resuspended in 3.5 ml of microsome resuspension buffer for TPP by pipetting and added to a 13.5-g phase system. The phase system was made up with microsome resuspension buffer for TPP to 18.0 g. After thorough mixing by vigourous shaking for 40 times and centrifugation at 2,000 x *g*, the primary upper and lower phases were obtained. The primary upper phase (enriched for right-side-out plasma membrane vesicles) was repartitioned twice with fresh lower phases. Likewise, the primary lower phase containing endomembranes and inside-out plasma membrane vesicles was repartitioned twice with fresh upper phases. Fresh phases were obtained by adding 4.5 g of microsome resuspension buffer to a 13.5-g phase system and shaking and centrifuging as described. The final upper and lower phases were diluted in 30 ml of PM washing buffer, and the membrane vesicles were pelleted by centrifugation at 180,000 x *g* for 30 min in a SW40Ti rotor (Beckman Coulter). Finally, the membranes from upper and lower phases were resuspended in 100 and 200 µl of PM washing buffer, respectively, and stored at -80°C. Equal portions of both samples were analysed by Western blotting (see 2.3.3) using antibodies for CPK3 and markers for the plasma membrane, the vacuolar membrane, the mitochondrial membrane, and the ER/Golgi (see 2.3.4).

2.3.9 Fractionation for Analysis of the Membrane Association of CPK3

To isolate the microsomal and soluble fraction, 6 g of leaves and roots were harvested from 8-weeks old hydroponically grown plants. The roots were washed with cold distilled water and well dried in paper towels. The material was quick-frozen in liquid nitrogen and grinded with mortar and pestle. Subsequently, it was mixed with 12 ml of pre-cooled homogenisation buffer with EDTA, vortexed and centrifuged at 10,000 x *g* for 20 min at 4°C in a SW40Ti

rotor (Beckman Coulter). Supernatant centrifuged again at 100,000 x *g* for 1 h at 4°C in the same rotor. Thereby, the microsomal and the soluble fraction were obtained as the pellet or supernatant, respectively.

The pellet was washed with homogenisation buffer with EDTA and resuspended in 200 µl of SDS-loading buffer by pipetting. The soluble fraction was subjected to acetone precipitation to concentrate its proteins. Therefore, 400 µl of the supernatant were mixed with 1600 µl of ice-cold aceton and incubated over night at -20°C. Then, the precipitated proteins were recovered by centrifuging for 10 min with 16,100 x *g* at 4°C. The supernatant was discarded, and the pellet was washed by adding 500 µl of ice-cold aceton, breaking the pellet with a tip and centrifuging for 5 min with 9,300 x *g* at 4°C. The supernatant was removed completely. The pellet was dried at 40°C for 2-5 min and resuspended in 30 µl of SDS-loading buffer.

Finally, equal proportions of both fractions according to their original volumes were analysed by Western blotting (see 2.3.3) in regard to the presence of CPK3. One times supernatant or pellet refers to a 0.8% of the original volumes.

2.4 Bacterial Methods

2.4.1 Bacterial Strains

DH5α: *Escherichia coli* strain used for cloning

F-, ø80dlacZDM15, D(lacZYA-argF)U169, deoR, recA1, endA1, sdR17 (rk,mk+), phoA, supE44, 1-, thi-1, gyrA96, relA1

AGL1: *Agrobacterium* strain used for transient protein expression in tobacco epidermal cells

AGL0 (C58pTiBo542) recA::bla, T-region deleted Mop(+) Cb(R)

2.4.2 Preparation of Chemically Competent *E. coli*

First, a preculture culture of freshly plated DH5α cells was prepared in 100 ml of LB medium complemented with 20 mM $MgSO_4$ and grown over night at 23°C. The preculture then was used to inoculate an overnight culture in 300 ml of LB medium complemented with 20 mM $MgSO_4$, which was grown at 23°C until the optical density at 600 nm of 0.6 was reached. The culture was cooled immediately, split into six Greiner flasks à 50 ml and incubated on ice for 10 minutes. To pellet the cells, the cultures were centrifuged at 700 x *g* for 10 min at 4°C. The pellets were resuspended in altogether 64 ml of pre-cooled transformation buffer by gentle shaking, pooled in two Greiner flasks and incubated on ice for 10-30 min. Subsequently, the suspensions were centrifuged at 400 x *g* for 10 min at 4°C.

The pellets were resuspended in altogether 16 ml of pre-cooled transformation complemented with 7% DMSO and incubated on ice for one to two hours. The cell suspensions were filled into Eppendorf tubes, freezed immediately in liquid nitrogen or dry ice and stored at -80°C.

2.4.3 Transformation of Chemically Competent *E.coli*

For one ligation, 50 µl of chemically competent *E. coli* cells were thawed on ice, added to the ligation mix (see 2.2.7) and incubated on ice for 30 min. The heat-shock was performed at 42°C for 60 s without shaking. Immediately after, the cells were briefly cooled on ice, and 1 ml of LB medium was added. For recovery, the suspension was incubated for 1 h at 37°C under shaking. Finally, the cells were pelleted by centrifuging at 16,100 x *g* for one minute at room temperature, resuspended in 100 µl of LB and dispersed on LB-plates supplemented with the appropriate antibiotics. The plates were incubated overnight at 37°C.

2.4.4 Transformation of Electro Competent *Agrobacteria*

50 µl of freshly thawed electro competent *Agrobacteria* cells (kindly provided by Bernhard Wurzinger and Simon Stael) were transferred to a 2 mm electroporation cuvette (EquiBio), carefully mixed with 0.5 µg of plasmid DNA and cooled on ice. The electroporation was done at 1.4 kV voltage, 25 µF capacitance and 200 Ω resistance (Pulse Controller and Gene Pulser from Bio-Rad). The cells were immediately mixed with 1 ml of LB, transferred to an Eppendorf tube and shaken for 1 h at 28°C for recovery. Subsequently, the suspension was centrifuged at 16,100 x *g* for 1 min at room temperature. The cells were resuspended in 100 µl of LB and dispersed on LB plates supplemented with the appropriate antibiotics. The plates were incubated at 28-30°C for 3 days. Transformation of clones was tested by PCR (see 2.2.8), and positive clones were used for infiltration of tobacco leaves (described in 2.6.4).

2.5 Yeast Methods

2.5.1 Yeast Strains

L 40: yeast strain used for yeast two-hybrid assays

MATα hisΔ200 trp1-900 leu2-3.112ade2 LYS :: (lexA op)$_4$HIS3 URA3 :: (lexA op)$_8$ lacZ Gal4 gal80

2.5.2 Transformation of Yeast (Quick Method)

For transformation of yeast, 150 µl of transformation mix was mixed with a considerable amount of L 40 yeast cells picked from a plate and supplemented with 2 µg of DNA per plasmid. The cells were incubated for 20 min at 30°C without shaking. The heatshock was performed at 44°C for 20 min without shaking. Then, the cells were mixed with 1 ml of water and pelleted by centrifugation at 5,900 x *g* for 1 min at room temperature. The pellet was resuspended in 100 µl of water and plated on SD-leu-trp plates to select for transformation with pBTM117 and pACTIIJ. The plates were closed with parafilm and incubated for 4 to 7 days at 30°C.

2.5.3 Protein extracts from Yeast

For preparation of protein extracts from yeast, an overnight culture was set up in 3 ml of SD-leu-trp by inoculating small amounts of several yeast colonies until a slight clouding was visible. The next day, 2 ml of the culture were centrifuged at 5,900 x *g* for 1 min at room temperature, the supernatant was removed, and 200 µl of enzyme lysis buffer together with 200 µl of glass beads was added to the pellet. The cells were immediately frozen in liquid nitrogen. After thawing, the cells were lysed by vortexing at 4°C for 20 min. To remove the cell debris, the suspension was centrifuged at 16,100 x *g* for 10 min at 4°C. The supernatant was transferred to a fresh Eppendorf tube and centrifuged again as previously. Finally, the supernatant constituting the protein extract was transferred to a fresh tube and cooled on ice.

2.5.4 β-Galactosidase Activity Assay

To determine the activity of β-galactosidase in yeast two-hybrid assays, 50 µl of protein extract (see 2.5.3) were mixed with 650 µl of Z buffer and 100 µl of ONPG solution (stat point). When the solution visibly had turned yellow, the reaction was stopped by adding 400 µl of 1 M Na_2CO_3 solution (endpoint). If no colour was visible, the reaction was stopped after 10 min. The extinction was measured at 420 nm and the total protein concentration was determined by the Bradford assay (see 2.3.6).

The specific activity of β-galactosidase [U/ mg of protein] was calculated as following with "time" being the time lag between start and end point:

Specific activity [U/mg protein] = E_{420nm} x 24 x 1000 / (45 x time [min] x protein conc. [mg/ml])

2.6 Plant Methods

2.6.1 Plant Lines

Col-0: wild-type *Arabidopsis thaliana* line ecotype Columbia

***cpk3-2*:** T-DNA insertion line, SALK_02286246, full *cpk3* ko line at mRNA and protein level (Mehlmer *et al.*, 2010)

***cpk3-1*:** *cpk3* knock-down line (Mehlmer *et al.*, 2010)

***cpk3-3*:** *cpk3* over-expressor line (Mehlmer *et al.*, 2010)

***tpk1*:** *tpk1* knock-out line obtained from Dirk Becker

SR1: wild-type *Nicotiana tabacum* line

2.6.2 Sterilisation of Seeds with Chlorine Gas

Open Eppendorf tubes filled with approximately 100 µl of seeds were laid horizontally into a plastic box that was laid out with green paper towels. Two 500-ml beakers were placed into the box, one filled with ~100 ml of bleach (1:1 diluted with water), the other filled with three spoons of $KMnO_4$. The reaction was started by adding ~50 ml of 5 M HCl to each of the two beakers. The plastic box was tightly closed immediately, and the generation of chlorine gas was monitored by the bleaching of the paper towels. After two hours, the plastic box was opened, and the Eppendorf tubes were closed quickly. To retain a high germination capacity, the chlorine gas was removed from the seeds by placing the open tubes into a sterile hood for a few hours. The sterilised seeds can be stored for a few months in a dark place at room temperature.

2.6.3 Cultivation of Plants

Agar-grown *Arabidopsis* plants:

Sterilised *Arabidopsis* seeds were dispersed on plates containing ½ MS medium. The plates were closed tightly with parafilm, and the seeds were vernalised at 4°C in the dark for 48 hours. The plates were incubated in a growth room with a 16 h light/ 8 h dark photoperiod, 22 +/- 5°C and with 100-150 µmol m^{-2} sec^{-1} light intensity applied by fluorescent tubes of the brands Polylux XL (F3GW/827) or Yellow Osram L (36W7827) or Lumoflor Navra LT 36W/077. To reduce generation of condensate due to heating of the plates by beneath lamps, the plates were incubated on the lowest shelf.

Hydroponically-grown *Arabidopsis* plants:

0.5 ml PCR tubes were completely filled with ½ MS medium supplemented with 0.5% plant agar and transferred to a cold room for solidifying. In the meantime, boxes for 1-ml tips were filled with 400 ml of Hoagland medium. The white inset was inserted inversely with the smooth side up, and the boxes were closed with aluminium foil. A 5-ml tip was used to punch four holes through the foil in the corners of the box. After solidifying, the tips of the PCR tubes were cut with a scissor, the lid of the tubes was removed, and non-sterilised seeds were placed individually on top of the medium (one seed per tube). The tubes were placed into the holes of the box. A 5-ml tip was plugged into the middle of the each box and cling film was wrapped around the boxes to produce a transparent hat for the boxes. Finally, the cling film was fixed with an elastic strap.

The boxes were transferred to a growth chamber with the same conditions as for agar-grown plants, but with an 8 h light/16 h dark photoperiod (short day).

The cling film was removed after approximately 3 weeks, and the plant material was harvested after 6 to 8 weeks.

Soil-grown tobacco and *Arabidopsis* plants:

Non-sterilised *Nicotiana tabacum* or *Arabidopsis* seeds were dispersed on Max-Planck-Soil (80 l contain 70 l of Spezialsubstrat "Max-Planck-Institut" from Stender, 75 g Osmocote Start from Scotts and 2 g Confidor from Bayer dissolved in 10 l of water). The seeds were watered well and protected against loss of water with a transparent plastic cap, which was removed after germination. Tobacco were grown for 6 weeks in a growth chamber with the same conditions as for agar-grown plants, but with an 8 h light/16 h dark photoperiod (short day). *Arabidopsis* plants were grown under short day as well, but transferred to long-day conditions (16 h light/ 8 h dark) after 6 weeks to induce shoot growth and generation of seeds. After observation of senescing leaves and fully-maturated siliques, the plants were not watered anymore. Seeds were harvested from fully-dried plants after altogether 10-12 weeks.

2.6.4 *Agrobacteria*-mediated Expression of Proteins in Tobacco Leaves

For transient expression of proteins in epidermal cells of tobacco leaves, *Agrobacterium* cells carrying the plasmid of desire were inoculated in 5 ml of LB medium supplemented with kanamycin (LB-kan) and grown overnight at 30°C under shaking. The next day, the culture was diluted in altogether 50 ml of LB-kan and was incubated at 30°C for another 3 h

under shaking. The cells were pelleted by centrifuging at 3,000 x *g* for 10 min at room temperature. The supernatant was discarded, and the cells were resuspended in 30 ml of LB supplemented with 150 µM acetosyringon. The culture was incubated again for 2 h at 30°C with shaking. The optical density at 600 nm was determined with a photometer, and the cells were pelleted as before. The cells were resuspended in water containing 5% sucrose in a way that a final optical density of 1.5 was reached. In case of co-expression of two proteins, the corresponding cultures were mixed 1:1. Using a 1-ml syringe, the *Agrobacterium* suspension was carefully infiltrated into young, pre-perforated leaves of 5 to 6 week old *N. tabacum* plants. A positive control (usually *Agrobacteria* carrying ntCFP-CPK3 together with ctCFP-TPK1) was infiltrated into each used leaf, and the other *Agrobacterium* suspensions were infiltrated into other sectors of the same leaf. The leaves were wetted with a water spray and dried again with paper towels. The plants were incubated overnight in an orange plastic bag at room temperature and transferred to a green house.

The expression of the proteins was visualised with a confocal fluorescence microscope (LSM or LSM meta from Zeiss) 40-48 h after infiltration. Therefore, small leaf pieces were cut out and vacuum infiltrated in a 50-ml syringe filled with 20 ml of water. The leaf pieces were laid upside down onto slides which were supplied with double-sided tape at the edges. The paper protecting the double-sided tape was removed, and small drops of water were carefully placed onto the leaves. Finally, a coverslip was laid onto the slides. The used laser lines were: 458 nm for excitation of CFP and chloroplasts and 561 nm for mCherry.

2.6.5 Quantification of Interaction with BiFC

Transient protein expression and microscopy was done as described in 2.6.4. As different leaves show considerably changing expression levels, all constructs were infiltrated into different sectors of the same leaf. At least five well-expressing leaves were selected for quantification. From each leaf and construct, 10 pictures of 2046 x 2046 pixels were taken with exactly the same settings from a randomly chosen area, only the focus was adjusted for optimal fluorescent signal. In each picture, the cell periphery where the interaction was visible was marked with the software LSM image browser with one pixel thickness, and the values corresponding to the signal strength of all marked pixels were obtained. Then, the mean signal strength per picture was calculated, followed by the mean of the mean signals per leaf. In case of the positive control (ntCFP-CPK3 + ct-CFP-TPK1), this value was set to 1. The mean signal strength values per leaf of the other combinations were calculated in

relation to the positive control. The normalised values from the five leaves were used to calculate the final normalised mean, and the standard deviation was obtained from the values of the different leaves.

2.6.6 Germination Assays

Seeds of different *CPK3* and *TPK1* knockout and overexpressing lines (see 2.6.1) were dispersed on plates as described in section 2.6.3. Three different media were used: (i) basal mineral medium (as described by Spalding *et al.*, 1999) supplemented with 2 mM KCl (control medium), (ii) basal mineral medium supplemented with 2 mM KCl and 150 mM NaCl (salt medium), and (iii) basal mineral medium supplemented with 50 µM KCl and 150 mM NaCl (low potassium and salt medium). Each line was dispersed on at least 3 control plates and 5 stress plates with approximately 100 seeds per plate. Germination was counted after 3, 4 and 7 days after placing into the light. A seed was considered as germinated as soon as the radicle was visible.

3 Results

3.1 CPK3 is Primarily Soluble but also Associates to Membranes

It has recently been demonstrated that CPK3 is involved in salt-stress acclimation (Mehlmer *et al.*, 2010). However, its precise function in this respect has not been identified yet. As the subcellular localisation provides a helpful insight into the function of a protein, I set out to study this aspect in more detail. Previously, it has been known from YFP/GFP-fusions in tobacco (Mehlmer *et al.*, 2010) and *Arabidopsis* (Dammann *et al.*, 2003) that CPK3 localises to the nucleus, to cellular membranes, and to the cytosol. The membrane association was confirmed with biochemical fractionation experiments as well, but the extent to which CPK3 was found in the cytosol in these studies was controversial. To unravel this mistery, I conducted a semi-quantitative fractionation experiment using roots and leaves from wild-type *Arabidopsis* plants. By centrifugation at 100,000 x *g* for 1 h, I obtained a soluble fraction containing soluble proteins (supernatant) and a microsomal fraction containing membrane-bound proteins (pellet). Equal portions of both fractions were analysed by Western blotting for the presence of CPK3 and the plasma membrane marker H^+-ATPase (Fig. 3.1.1). H^+-ATPase was detected only in the microsomal fraction (10x or 5x pellet), indicating that the supernatant contains exclusively soluble proteins and is not contaminated with microsomes (Fig. 3.1.1A). The CPK3-specific antibody revealed that CPK3 is found in both fractions (Fig. 3.1.1B). In roots and leaves, approximately four times more CPK3 was detected in the soluble fraction than in the microsomal fraction, as the signal strength obtained from the two-times (2x) pellet was similar to that of the half-time (½x) supernatant. This result indicates that the major part of cellular CPK3 is soluble and not associated with membranes.

As a soluble protein is not mandatorily a cytosolic protein but may also be located in organelles such as the nucleus, I analysed the subcellular localisation of CPK3 fused to YFP (CPK3-YFP) in tobacco epidermal cells as has been previously done by Mehlmer *et al.* (2010). In these cells, the vacuole is the dominant organelle that pushes the cytosol and the nucleus to the very edges of the cell (Fig. 3.1.2A). Accordingly, the discrimination between a cytosolic localisation and association to plasma membrane or tonoplast is difficult. In rare cases, however, the vacuole peels off the cell edges, giving rise to cytosolic lobes. These allow to distinguish between a cytosolic and non-cytosolic localisation.

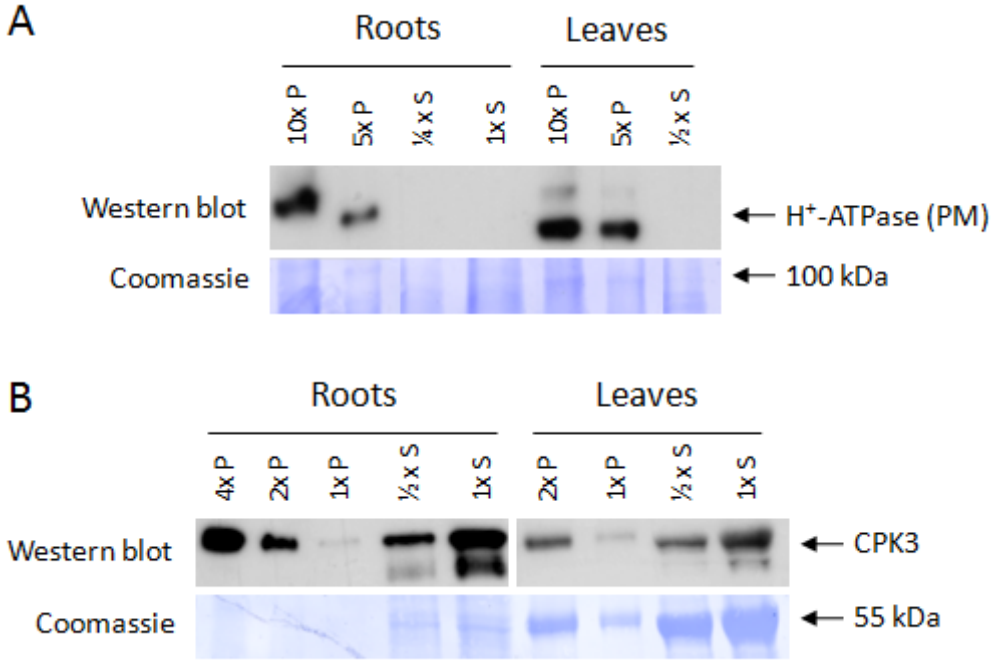

Figure 3.1.1. CPK3 is a primarily soluble protein but also associates to membranes. A microsomal (P, pellet) and a soluble fraction (S, supernatant) were obtained from wild-type roots and leaves by centrifugation at 100,000 x *g* for 1 h. Equal proportions of both fractions were subjected to Western blotting (upper panels) with antibodies specific for H^+-ATPase (marker for the plasma membrane, *A*) and CPK3 (*B*). Total proteins were stained with coomassie (lower panels). One time (1x) supernatant and pellet refer to 0.8% of the original volumes. PM, plasma membrane.

CPK3-YFP localises to cytosolic lobes, demonstrating its cytosolic distribution (Fig. 3.1.2B, C, D). As observed before, CPK3-YFP signals are also detected in the nucleus and at the cell periphery, which is likely to represents a membrane association. Taken together, these results demonstrate that CPK3 is a primarily soluble protein that localises to the nucleus and to the cytosol and associates to membranes only partially.

3.2 Analysis of Membrane Association of CPK3

The nuclear localisation of CPK3 would suggest a role in transcriptional reprogramming, i.e. a CPK3-dependent induction of stress-related genes. However, this was not detected in response to salt stress (Mehlmer *et al.*, 2010). It has therefore been suggested that CPK3 could be involved in the direct regulation of ion channels or transporters to re-establish cellular ion homeostasis (Mehlmer *et al.*, 2010). As this is closely linked to the membrane association of CPK3, I set out to analyse this aspect in more detail.

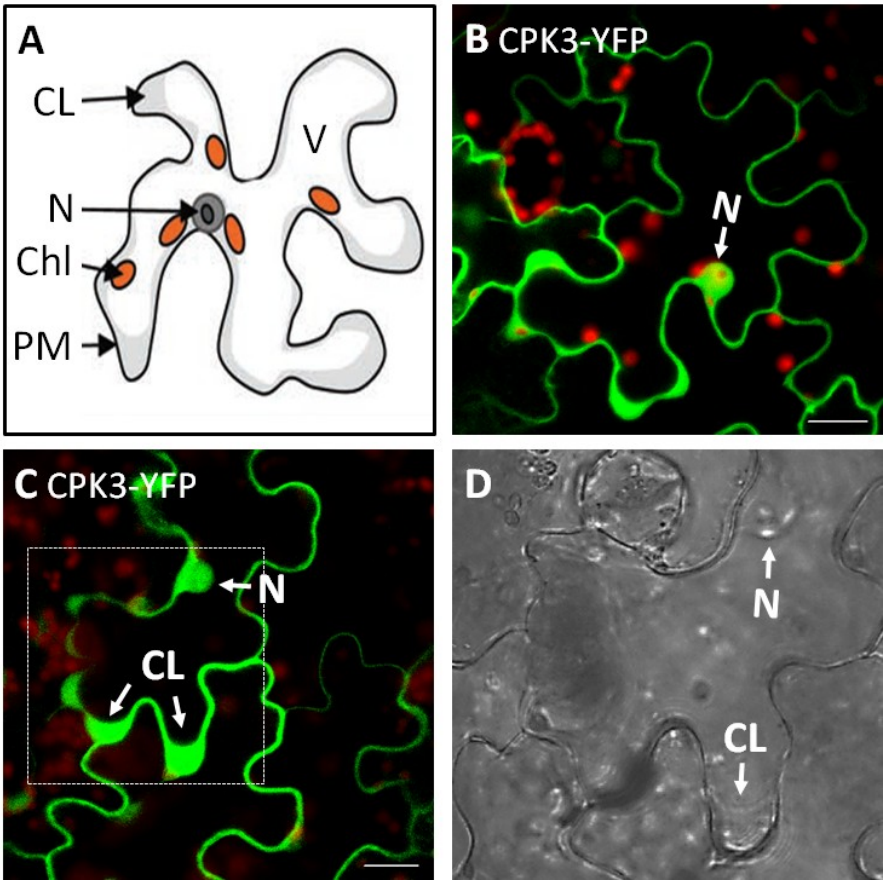

Figure 3.1.2. Subcellular localisation of CPK3-YFP in tobacco epidermal leaf cells. CPK3-YFP was transiently expressed under the 35S promoter from cauliflower mosaic virus by *Agrobacterium*-mediated transformation. (A) Schematic presentation of an epidermal leaf cell (adapted from Benetka *et al.*, 2008). (B,C) Merged pictures from the CPK3-YFP signal (green) and the signal obtained from autofluorescence of chloroplasts (red). (D) Bright field image and enlargement of the rectangle shown in *C*. Note the clearly visible cytosolic lobe (CL). The white bar indicates 20 µm. CL, cytosolic lobe; N, nucleus; Chl, chloroplast; PM, plasma membrane; V, vacuole.

To investigate whether CPK3 is attached to the plasma membrane, I isolated plasma membrane vesicles from leaves by aqueous two-phase partitioning. This technique is based on two immiscible polymer phases to which distinct membranes preferentially partition according to their surface properties (Santoni, 2007). Whereas all endomembranes as well as inside-out plasma membrane vesicles partition in the lower phase, solely right-side-out (apoplastic-side-out) plasma membrane vesicles prefer the upper phase, leading to an enrichment of plasma membrane in the upper phase (Larsson, 1994). To analyse the composition of the two phases, the presence of membrane markers was analysed by Western blotting with antibodies specific for these proteins (Fig. 3.2.1A). In the upper phase, only the plasma membrane marker (H^+-ATPase) was detected, indicating that the obtained plasma membrane is highly pure. CPK3 was detected in the upper phase as well, which demonstrates its association with the plasma membrane in leaves.

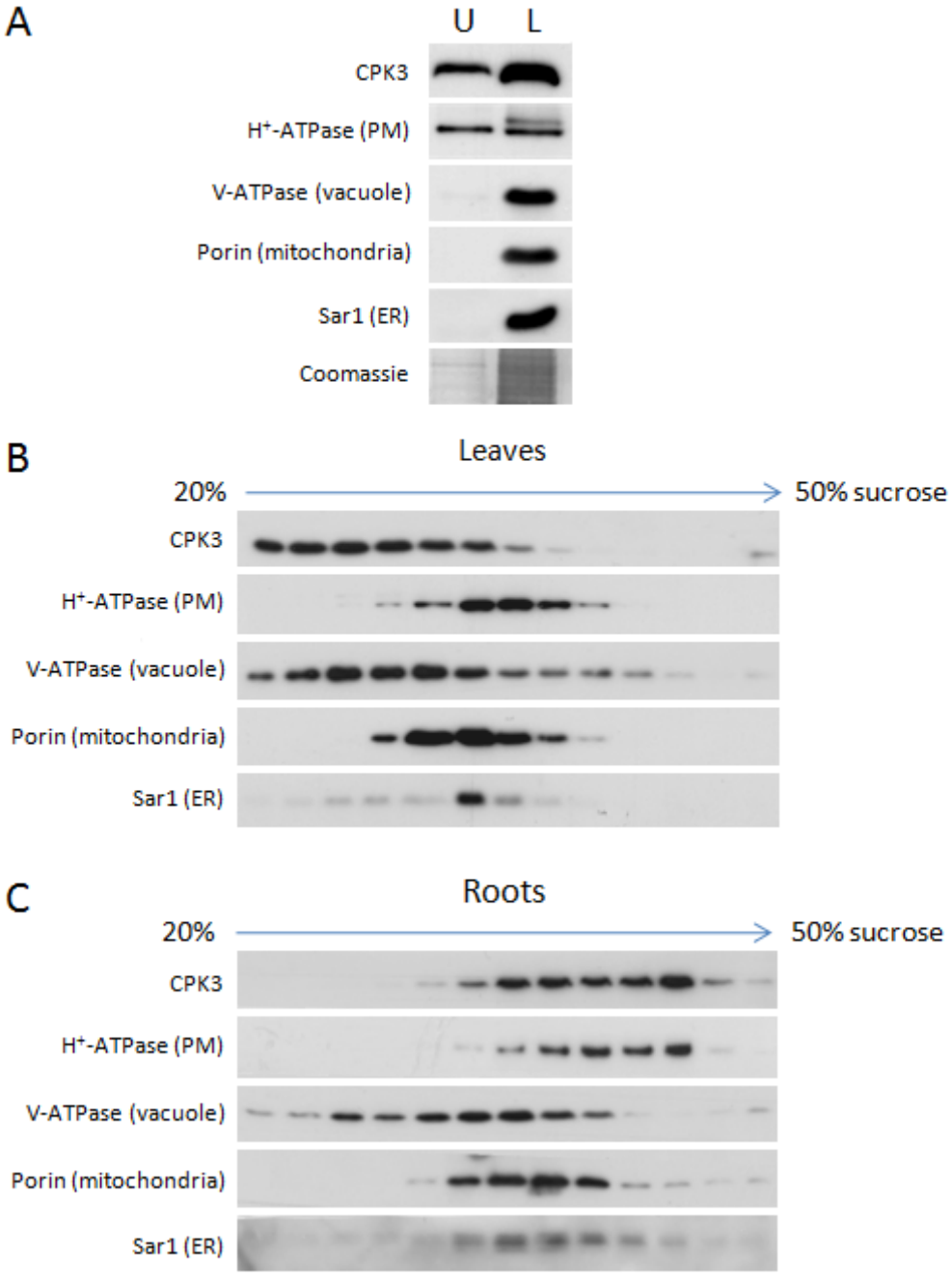

Figure 3.2.1. Analysis of the membrane association of CPK3. (A) Microsomal membranes from leaves from *Arabidopsis* wild-type plants were subjected to aqueous two-phase partitioning. The upper phase (U) and lower phase (L) consisted of polyethylenglycol (PEG) 3,350 or dextran T-500, respectively. The presence of membranes in the upper phase (which enriches right-side-out plasma membrane vesicles) and lower phase (which contains all endomembranes as well as inside-out plasma membrane vesicles) was analysed with Western blotting using antibodies specific for the H^+-ATPase (plasma membrane), the V-type ATPase (vacuolar membrane), a porin (outer mitochondrial membrane), and Sar1 (ER/Golgi). CPK3 was detected with a CPK3-specific antibody. (B, C) Separation of membranes on sucrose gradients. Microsomal membranes from leaves (B) and roots (C) from *Arabidopsis* wild-type plants were separated according to their density on linear sucrose gradients. Membranes and CPK3 were detected as described in *B*. U, upper phase; L, lower phase; PM, plasma membrane;

Interestingly, a considerably stronger signal from the CPK3-specific antibody was observed in the lower phase, where similar amounts of plasma membrane but also endomembranes are found. This indicates that CPK3 is additionally associated with at least one endomembrane in leaves.

To analyse this further, microsomal membranes from roots and leaves were separated according to their *buoyant* density on linear sucrose gradients. Again, the presence of membranes was analysed by Western blotting with antibodies against membrane-specific markers and compared to the distribution of CPK3 (Fig. 3.2.1B, C). In leaves, CPK3 was found to partially co-migrate with the plasma membrane but most of CPK3 co-migrated with the vacuolar membrane, indicating that CPK3 is attached to the tonoplast (Fig. 3.2.1B). Unexpectedly, a different distribution of CPK3 was observed in roots. Here, CPK3 was repeatedly detected in the high-density fractions co-migrating with the plasma membrane but only weakly in low-density fractions which contain vacuolar membrane (Fig. 3.2.1C). Thus, in roots CPK3 is primarily associated with a high-density membrane, most likely the plasma membrane. In leaves, however, CPK3 is largely attached to the vacuolar membrane and only to a lesser extent with the plasma membrane.

3.3 Analysis of the Interaction Between CPK3 and its Putative Targets by BiFC

Recently, a proteomics approach has identified several putative targets of CPK3 (Mehlmer *et al.*, 2010). In this experiment, microsomal membranes isolated from a root suspension culture were incubated with radiolabelled ATP and recombinant CPK3, and the proteins were separated by 2D gels according to their isoelectric points (IEP) and molecular weights. Proteins in radiolabelled spots were then identified by mass spectrometry. To eliminate false candidates, the IEP and molecular weight of the identified proteins were compared to the values in the original spots, and proteins with inconsistency were not further considered. The remaining candidates were ranked according to the occurrence of CDPK phosphorylation consensus sites (Table 1, Mehlmer *et al.*, 2010). However, as no direct evidence for the phosphorylation of these putative targets by CPK3 was provided by this approach, they need to be investigated further.

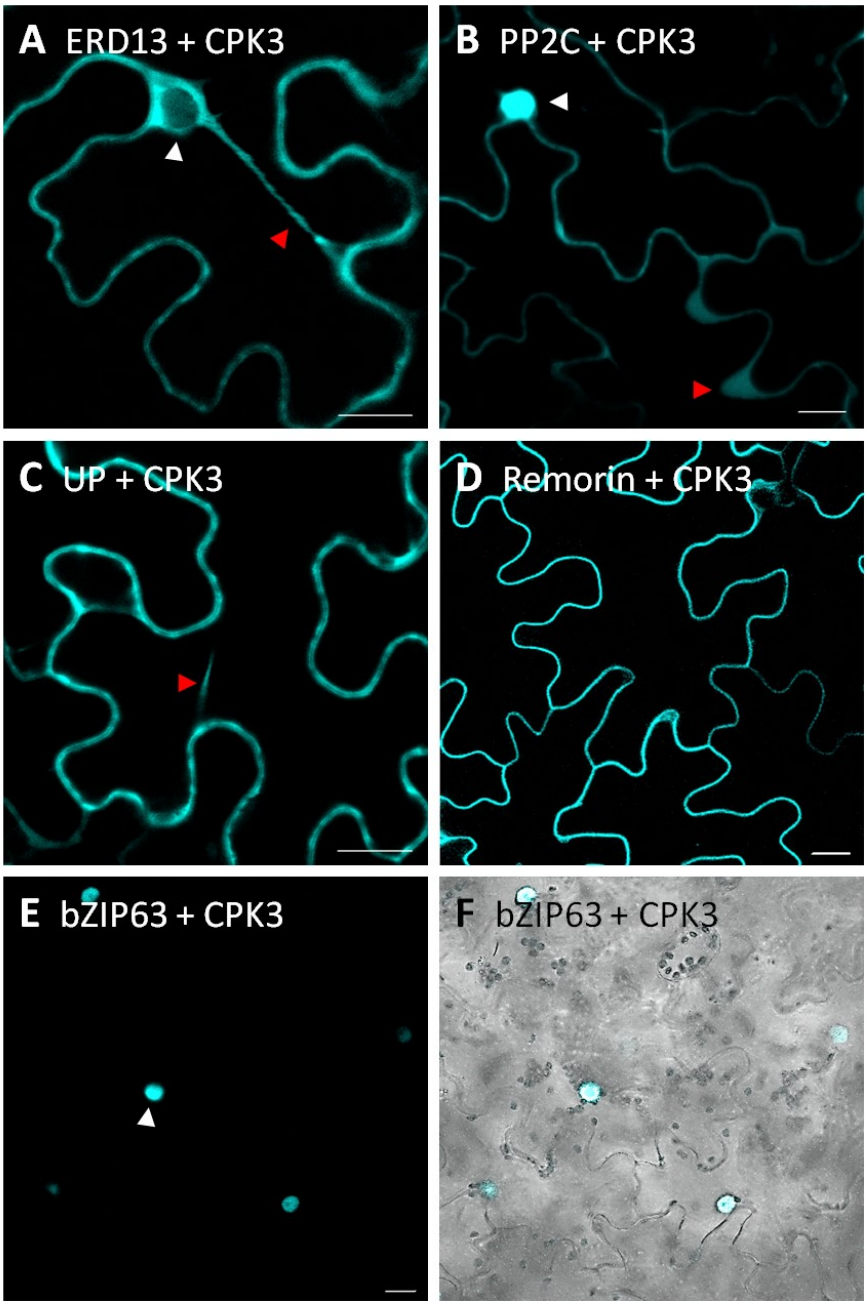

Figure 3.3.1. Interaction between CPK3 and its putative targets revealed by BiFC. ntCFP-CPK3 was transiently co-expressed with ctCFP-ERD13 (A), ctCFP-PP2C (B), ctCFP-UP (unknown protein, C), and ctCFP-Remorin (D) in tobacco epidermal cells by *Agrobacterium*-mediated transformation. Similarly, CPK3-ctCFP was coexpressed with ctCFP-bZIP63 in *E* and *F*. The CFP channel is shown exclusively (A-E) or together with the bright field (F). White and red arrows indicate nuclei and cytosolic lobes/strands, respectively. The white bar indicates 20 µm. ctCFP, C-terminal half of CFP; ntCFP, N-terminal half of CFP; UP, unknown protein.

To analyse whether the putative targets interact with CPK3, I conducted bimolecular fluorescence complementation (BiFC) experiments (Waadt *et al.*, 2008). As the most promising candidates I selected the glutathione-*S*-transferase ERD13 (AT2G30870), the remorin protein (AT2G45820), the regulating channel subunit KAB1 (AT1G04690), the protein of unknown function (AT3G18240; unknown protein, UP), the Ca^{2+} binding proteins calreticulins CRT1 (AT1G56340) and CRT2 (AT1G09210), and the PP2C-type phosphatase (AT3G02750; PP2C) (Table 1). CPK3 was fused to ntCFP and the putative targets were fused to ctCFP (both either N- or C-terminally), and these constructs were transiently co-expressed in tobacco epidermal cells. In initial experiments, all four possible combinations of N- or C-terminal fusions were tested on the same leaf, and the best combination was selected for further analysis. A relatively strong fluorescent signal was observed upon co-expression of ntCFP-CPK3 together with ctCFP-ERD13 (Fig. 3.3.1A), ctCFP-PP2C (Fig. 3.3.1B), the unknown protein fused to ctCFP (Fig. 3.3.1C), and ctCFP-remorin (Fig. 3.3.1D), indicating that these proteins interact with CPK3 *in planta*. Interestingly, these interactions were observed at different subcellular localisations, which is consistent with the versatile localisation of CPK3. The interaction between CPK3 and ERD13 and the unknown protein was observed in the cytosol, as signals in cytosolic strands and in the cytosol around the nucleus were visible, and possibly also at cellular membranes. In case of PP2C and CPK3, the strongest signal was detected in the nucleus, but weak signals were also observed in cytosolic lobes. In contrast, the interaction between remorin and CPK3 was exclusively seen at the cell periphery, most likely at the plasma membrane where remorins have been previously shown to be localised (Raffaele *et al.*, 2007).

Very weak fluorescent signals were observed in case of calreticulin 1 and 2 (data not shown) and KAB1 together with CPK3 (Fig. 3.3.2A), indicating that these proteins do not interact with CPK3 *in vivo*. As shown for KAB1, a signal was gained by opening the pinhole widely to obtain fluorescent signals from other planes of the sample, increasing the background haze and the detection of signals from chlorophyll autofluorescence (Fig. 3.3.2B). However, under more stringent conditions similar to those used for the other putative targets, almost no fluorescent signal from KAB1 and CPK3 was observed (Fig. 3.3.2A). In contrast, a good fluorescence was detected under exactly the same conditions between CPK3 and TPK1, which is another putative target of CPK3 described in section 3.7 (Fig. 3.3.2C). To compare the expression levels of the involved proteins, I performed Western blot analysis with antibodies specific for the FLAG-tag of CPK3 or the HA-tag of KAB1 and TPK1.

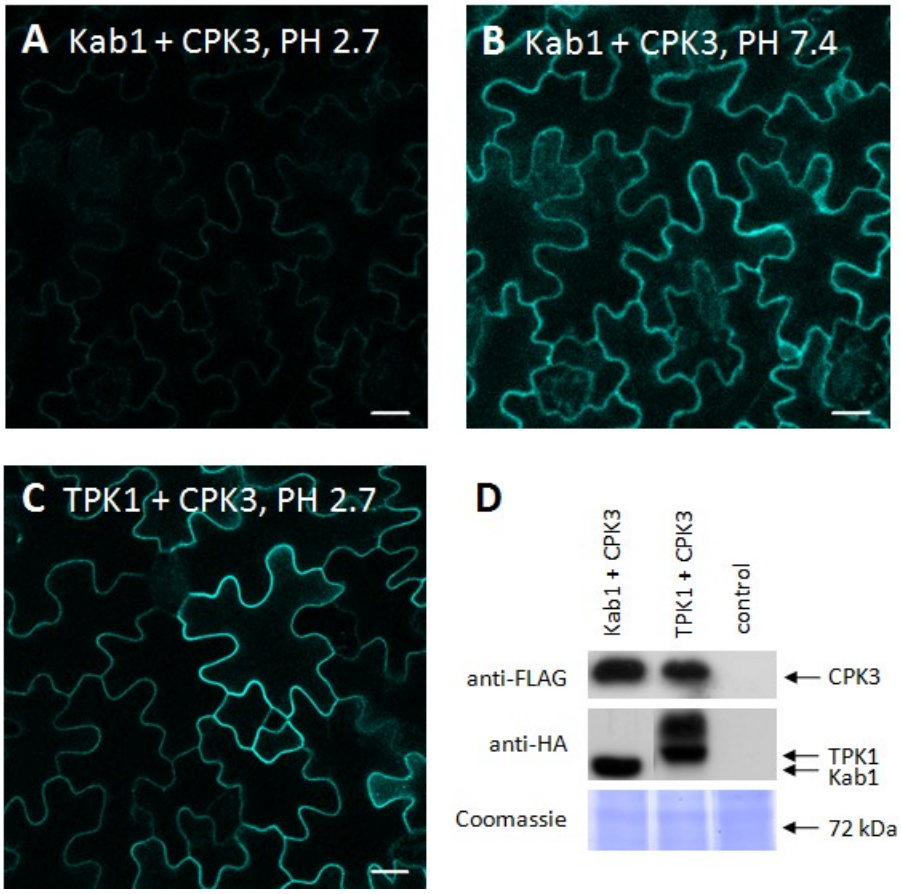

Figure 3.3.2. KAB1 does not interact with CPK3 in BiFC. ntCFP-CPK3 was transiently co-expressed with ctCFP-KAB1 (A, B) or ctCFP-TPK1 (C) in tobacco epidermal cells by *Agrobacterium*-mediated transformation. The CFP channel is shown exclusively. The pictures shown in *A* and *C* were taken under exactly the same conditions with a rather closed pinhole (PH) of 2.7. In *B*, the pinhole was opened to 7.4, which increases the fluorescent signal but results in background haze and fluorescent signals from the chloroplasts. The white bar indicates 20 µm.
(D) Western blot analysis using an anti-FLAG antibody against the FLAG-tagged ntCFP-CPK3 (upper panel) and an anti-HA antibody against the HA-tagged ctCFP-KAB1 and ctCFP-TPK1 (middle panel). Control is a protein extract from a non-infiltrated (non-transformed) tobacco leaf. The coomassie staining is shown in the lower panel. The expected protein sizes are 50 kDa and 51 kDa in case of ctCFP-KAB1 and ctCFP-TPK1, respectively. ctCFP, C-terminal half of CFP; ntCFP, N-terminal half of CFP, PH, pinhole.

Whereas no signals at the corresponding molecular weights were detected in the non-infiltrated control, equal signals of CPK3 and KAB1 or TPK1 were observed in both samples, suggesting similar expression levels. Thus, is likely that the weak fluorescence in BiFC of KAB1 together with CPK3 results from insufficient interaction between these two proteins. Taken together, these results indicate that CPK3 interacts with ERD13, PP2C, the unknown protein and remorin *in vivo*, but not with calreticulin 1 and 2 and KAB1.

3.4 The Specificity of BiFC Experiments

In order to analyse the specificity of the observed interactions, four proteins with different subcellular localisations were selected and tested for their interaction with CPK3 using BiFC. These were (i) AP2C1, a PP2C-type phosphatase, which has been shown to interact with the MAP kinases MPK4 and 6 in the nucleus and cytoplasm (Schweighofer *et al.*, 2007); (ii) the cytosolic form of GAP dehydrogenase, GAPC-1 (Rius *et al.*, 2008); (iii) NHX1, which is a Na^+/H^+ antiporter at the tonoplast (Sottosanto *et al.*, 2007); and (iv) SOS1, a Na^+/H^+ antiporter at the plasma membrane that was not activated by CPK3 in a functional complementation assay in yeast (Mehlmer, 2008) and is therefore unlikely to interact with CPK3.

As described previously, CPK3 fused to ntCFP and the protein of interest fused to ctCFP were transiently co-expressed in tobacco epidermal cells, and the fluorescent signal was determined by confocal fluorescence microscopy. Surprisingly, co-expression of AP2C1 and GAPC-1 together with CPK3 resulted in robust fluorescence in the nucleus and cytosol, respectively, indicating that these two proteins interact with CPK3 in BiFC assay as well (Fig. 3.3.1). In case of NHX1 and SOS1, the interaction with CPK3 could not be analysed, as both proteins repeatedly failed to be expressed in tobacco leaves (data not shown). Thus, more data is necessary to evaluate the specificity of BiFC.

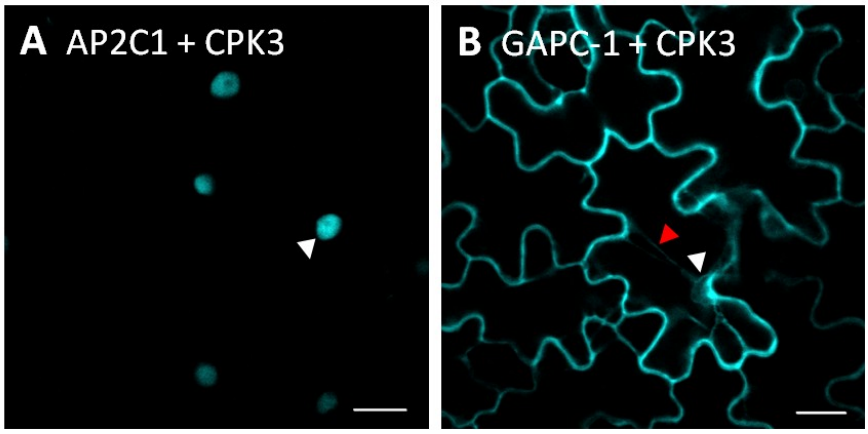

Figure 3.3.1. AP2C1 and GAPC-1 interact with CPK3 in BiFC assays. ntCFP-CPK3 was transiently co-expressed with ctCFP-AP2C1 (A) or ctCFP-GAPC-1 (B) in tobacco epidermal cells by *Agrobacterium*-mediated transformation. The CFP channel is shown exclusively. White or red arrows indicate nuclei and cytosolic strands, respectively. The white bar indicates 20 µm. ctCFP, C-terminal half of CFP; ntCFP, N-terminal half of CFP.

3.5 Interaction Between CPK3 and its Putative Targets in Yeast Two-Hybrid Assays

To assess the interaction between CPK3 and its putative targets with a second approach, I conducted yeast two-hybrid assays. As prey, I used CPK3dC K/R. This modified form of CPK3 lacks its C-terminal autoinhibitory domain, allowing substrate binding in the absence of Ca^{2+} signals. In addition, the replacement of Lys in position 107 by Arg (K/R) renders CPK3 kinase-inactive, which may therefore prolong the interaction between kinase and target (Mehlmer, 2008). The putative targets that had been analysed for interaction with CPK3 in BiFC studies (see 3.3) were used as baits in their wild-type forms. AP2C1 and GAPC-1, which had turned out to interact with CPK3 in BiFC assays, were tested as well. As a positive control, I used bZIP63 with CPK3 as this bZIP transcription factor has previously been shown to interact with CPK3 in yeast two-hybrid assays (Hofmann-Rodrigues, 2007) and also interacts with CPK3 in BiFC assys (Fig. 3.3.1E). The yeast two-hybrid assay was performed in the yeast strain L40, in which an interaction of the proteins fused to the DNA-binding domain (BD) and to the activation domain (AD), respectively, leads to the expression of β-galactosidase, which can easily be detected and quantified by a β-galactosidase assay.

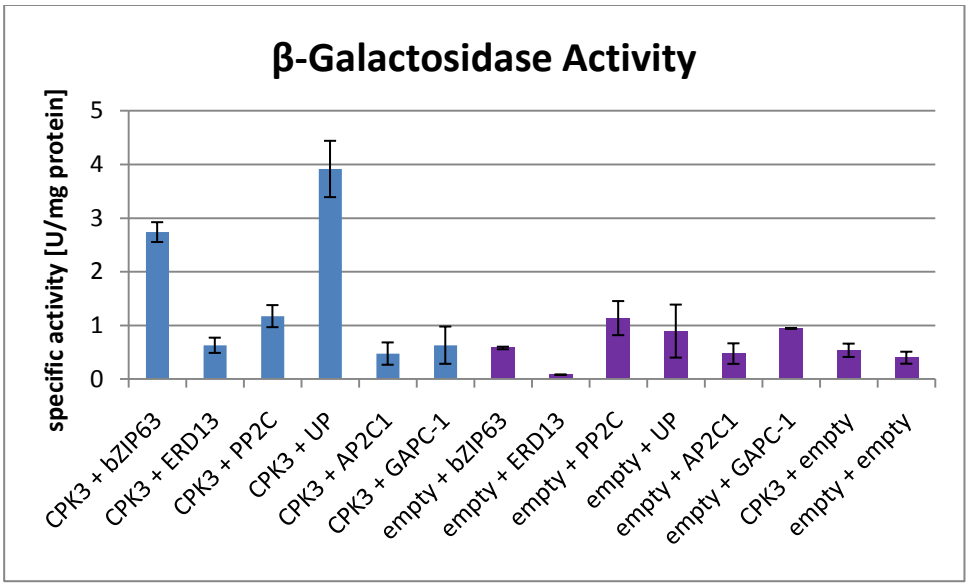

Figure 3.5.1. Results of the yeast two-hybrid assays. Quantitative β-galactosidase activity measurements using CPK3dC K/R fused to the activating domain (in pACTIIJ) and bZIP63, ERD13, PP2C, the unknown protein, AP2C1 or GAPC fused to the DNA-binding domain (in pBTM117). Values below 0.7 U/mg represent background activities. Controls are shown in violet. "Empty" means a control where a pBTM117 or pACTIIJ without insert was co-expressed. In the controls, two overnight cultures were tested (n=2), in all other cases three (n=3). Shown are mean values with standard deviations (error bars).

In line with the results from BiFC studies, no β-galactosidase activity was observed upon co-expression of calreticulin 1 and 2 and KAB1 together with CPK3 (data not shown). Remorin and CPK3 failed to induce expression of β-galactosidase as well, which was expected due to the membrane localisation of remorins (Raffaele *et al.*, 2007; Fig. 3.6.1C). Surprisingly, among the proteins that interacted with CPK3 in BiFC studies, only the unknown protein interacted with CPK3 in yeast (Fig. 3.5.1). This protein also showed a weak autoactivating activity. These results question the observed interaction from BiFC and demonstrate that further evaluation of these interactions is required.

3.6 Localisation of Putative Targets of CPK3

Previous results from BiFC have suggested that ERD13, PP2C, remorin and the unknown protein interact with CPK3 *in planta*. Microscopic analysis of the interacting complexes revealed different subcellular localisations from nuclear and cytosolic localisation to membrane association (Fig. 3.3.1). To analyse the localisation of these proteins independently of CPK3, I transiently expressed these proteins as C-terminal mCherry fusion proteins in tobacco epidermal leaf cells (Fig. 3.6.1). ERD13-mCherry showed a clear cytosolic localisation, as signals in cytosolic lobes and strands were observed, together with a weak nuclear localisation. This distribution is similar to the one of the CPK3-ERD13 complex (Fig. 3.3.1A). PP2C-mCherry was predominantly found in the nucleus and to a lesser extent in cytosolic areas, which is consistent with the BiFC results as well. Remorin-mCherry was detected at the cell periphery, most likely at the plasma membrane. Differently to the observation of remorin in complex with CPK3, remorin-mCherry was also found at cytosolic strands. However, this is likely to be an overexpression artefact since this aspect was more pronounced in strongly expressing cells. Thus, the mCherry fusion proteins of ERD13, PP2C and remorin showed a similar localisation as their counterparts in CPK3 complexes.

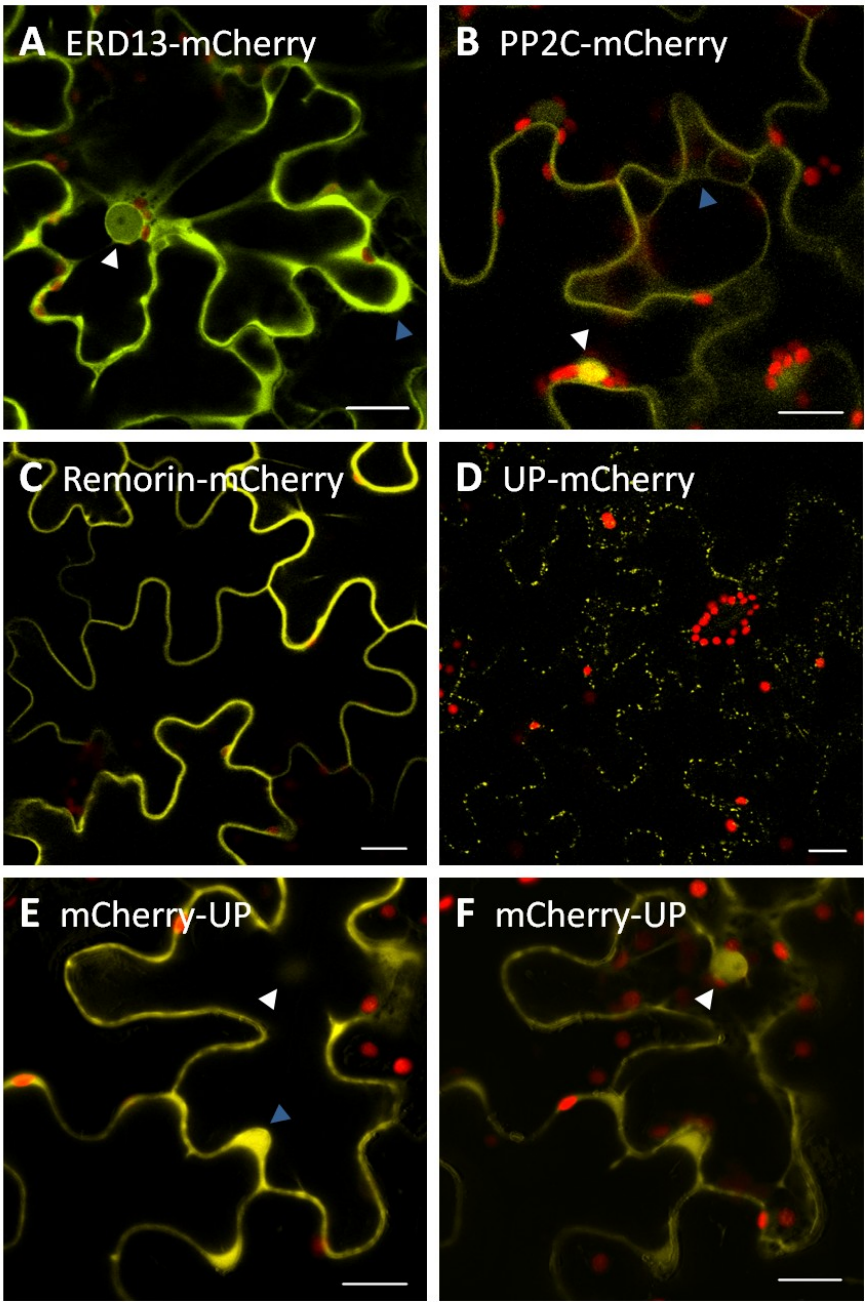

Figure 3.6.1. Subcellular localisation of mCherry fusion proteins in tobacco epidermal leaf cells. Merged pictures from the mCherry-fusion protein signal (yellow) and the signal obtained from autofluorescence of chloroplasts (red). ERD13-mCherry (A), PP2C-mCherry (B), Remorin-mCherry (C), UP-mCherry (D), and mCherry-UP (E, F) were transiently expressed under the 35S promoter from cauliflower mosaic virus by *Agrobacterium*-mediated transformation. (E, F) Differently focused images from the same cell. The white and blue triangles indicate nuclei or cytosolic lobes/strands, respectively. The white bar indicates 20 µm. UP, unknown protein.

In contrast, fusion of mCherry to the C-terminus of the unknown protein resulted in punctuate fluorescent signals that had not been observed in BiFC with CPK3 (Fig. 3.6.1D). Most likely, these structures represent mitochondria or oil bodies, which are small organelles filled with triacylglycerols (Galili *et al.*, 1998). The mitochondrial localisation was further

supported by bioinformatic analysis with ARAMEMNON (Schwacke *et al.*, 2003), which strongly predicted this localisation. However, co-localisation experiments in tobacco epidermal cells with a mitochondrial marker have repeatedly failed due to the relatively weak expression of UP-mCherry.

The surprising localisation of UP-mCherry raises the question how an interaction with CPK3 could be observed by BiFC (Fig. 3.3.1C). In these experiments, a fluorescent signal was detected only if the C-terminal half of CFP (ctCFP) was fused to the N terminus of the unknown protein, but not in case of C-terminal fusions. Therefore, I reasoned that the N-terminal fusion in the BiFC constructs might have masked its localisation signals leading to a distorted subcellular localisation. To test this hypothesis, I fused mCherry to the N terminus of the unknown protein and analysed its subcellular localisation in tobacco epidermal cells (Fig. 3.6.1E, F). In fact, this construct localised to the cytosol as seen by cytosolic lobes and to the nucleus, which is consistent with the localisation of its CPK3-complex in BiFC (Fig. 3.3.1C). Taken together, these results indicate that CPK3 and the protein of unknown function are able to interact, but this interaction presumably does not occur *in vivo* due to completely different subcellular localisations of the involved proteins.

3.7 TPK1, a Vacuolar K^+ Channel, Interacts With CPK3 *in planta*

TPK1 is a vacuolar two-pore potassium channel (TPK). Recently, it has been shown by ectopic expression in yeast that the activity of TPK1 is dramatically increased by binding to 14-3-3 proteins, which is favoured by phosphorylation of Ser42 in the 14-3-3 binding motif (Latz *et al.*, 2007). Kinase assays with cytosolic and microsomal protein extracts have revealed that TPK1 is effectively phosphorylated by a soluble Ca^{2+}-dependent kinase activity (Latz *et al.*). This indicates the involvement of soluble CDPKs such as CPK3 in the phosphorylation of TPK1. Moreover, a phosphorylation of TPK1 at Ser42 by CPK3 has been reported *in vitro* (Mehlmer, 2008).

To investigate whether TPK1 interacts with CPK3 *in planta*, I conducted BiFC experiments in tobacco epidermal cells. Co-expression of ntCFP-CPK3 and ctCFP-TPK1 resulted in a robust fluorescent signal, indicating an interaction *in vivo* (Fig. 3.3.2C). Consistent with the vacuolar localisation of TPK1 (Latz *et al.*, 2007), the signal was exclusively observed at membranes at the cell periphery but not in the cytosol.

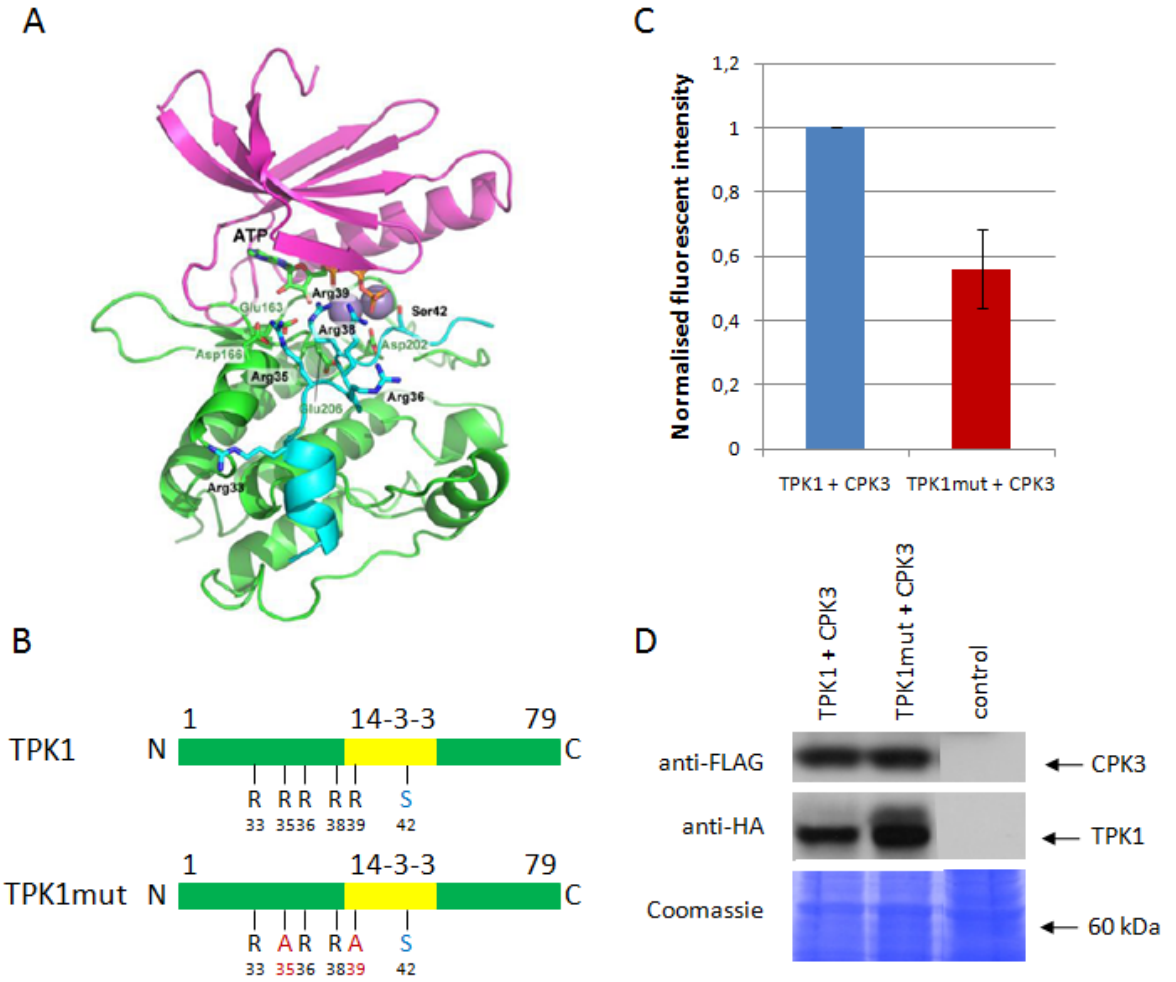

Figure 3.7.1. Interaction of TPK1 with CPK3 involves arginines 35 and 39 in TPK1. (A) Molecular modelling of the interaction between CPK3 and the N terminus of TPK1. CPK3 is shown in magenta or green, TPK1 is coloured blue. ATP and the magnesium ions are depicted as sticks and spheres, respectively (Latz *et al.*). (B) Schematic representation of the cytosolic N terminus (amino acids 1-79) of TPK1 in its wild-type (upper panel) or mutated form (lower panel). Both forms were used for BiFC studies in *C* and *D* in their full-length forms. The 14-3-3 binding site is coloured yellow. Ser42, which is phosphorylated by CPK3, is shown in blue. Point mutations introduced into TPK1 are coloured red. Numbers indicate the positions of the amino acid residues. (C) Quantification of interaction between ntCFP-CPK3 and ctCFP-TPK1 or ctCFP-TPK1mut. Both TPK1-constructs were co-expressed with ntCFP-CPK3 in tobacco leaves. The mean intensity fluorescent signal obtained from ctCFP-TPK1mut was normalised to the signal from ctCFP-TPK1. Error bars show standard deviation. (D) Western blot analysis using an anti-FLAG antibody against the FLAG-tagged ntCFP-CPK3 (upper panel) and an anti-HA antibody against the HA-tagged ctCFP-TPK1 and ctCFP-TPK1mut (middle panel). Control is a protein extract from a non-infiltrated (non-transformed) tobacco leaf. The coomassie staining is shown in the lower panel. ctCFP, C-terminal half of CFP; ntCFP, N-terminal half of CFP.

Structural modelling of the TPK1/CPK3 interaction implies that the multiple arginines close to the phosphorylation site Ser42 in the 14-3-3 binding site of TPK1 are involved in the recognition of CPK3 (Fig. 3.7.1A, B; Latz *et al.*). These positively charged residues are likely to bond with negatively charged glutamates/aspartates in CPK3, allowing a tight positioning of TPK1 in the substrate binding pocket of CPK3 (Latz *et al.*). We reasoned that

if these Arg are important for binding to CPK3, a replacement by Ala should dampen the interaction observed in BiFC assays. To test this hypothesis, I created a TPK1 mutant, in which Arg35 and Arg39 are substituted by Ala (TPK1mut), together with B. Wurzinger (Fig. 3.7.1B). In BiFC analysis with CPK3, a fluorescent signal was still observed in the TPK1 mutant, but seemed to be weaker (data not shown).

To assess the extent of this observed loss in interaction in more detail, we designed a method to quantify fluorescent signals obtained by BiFC. A major problem was the considerable variation of transient protein expression levels from leaf to leaf, which turned out to strongly influence the fluorescent signal. To circumvent this obstacle, we tested how these parameters fluctuate within a *single* leaf. In fact, fluorescent signals of BiFC were statistically equal in different sectors of a single leaf, allowing a direct comparison of fluorescent signals in case of different protein combinations (Bernhard Wurzinger, personal communication). Accordingly, ntCFP-CPK3 together with either ctCFP-TPK1 or ctCFP-TPK1mut was infiltrated into different sectors between bigger veins on the same leaf. Several pictures of randomly chosen areas were taken of each construct, and the mean signal strength was calculated. In the ctCFP-TPK1mut, the fluorescent signal upon co-expression with ntCFP-CPK3 was reduced by more than 40% compared to wild-type TPK1 (Fig. 3.7.1C). Western blot analysis revealed that expression levels of the involved proteins are approximately equal in both samples (Fig. 3.7.1D). Accordingly, the lowered fluorescent signal upon mutation of TPK1 is likely to be due to a reduced interaction between TPK1mut and CPK3. Taken together, these results demonstrate that TPK1 interacts with CPK3 *in vivo*, and that this interaction involves two Arg near to the 14-3-3 binding site of TPK1.

3.8 Physiological Function of the Interaction Between CPK3 and TPK1

To analyse the role of CPK3 and TPK1 in cellular K^+ homeostasis under salt stress, I analysed the germination of *cpk3* and *tpk1* lines on salt medium with and without K^+ starvation together with Bernhard Wurzinger (Fig. 3.8.1). We used a *tpk1* knock-out (*tpk1*) line provided by Dirk Becker and three different *cpk3* lines which had been analysed previously by Mehlmer *et al.* (2010). *cpk3-2* and *cpk3-1* are *cpk3* knock-out and knock-down lines, and *cpk3-3* is a CPK3-overexpressor. Under control conditions without salt stress and optimal K^+ levels, all lines germinated to 100% except for wild-type seeds, which had problems with survival, indicating that these seeds are in a generally bad state (Fig. 3.8.1, control). When grown on medium with severe salt stress (150 mM NaCl), the knock-

out/knock-down lines *cpk3-2*, *cpk3-1* and *tpk1* germinated similarly as the wild-type line. This is either due to redundancies in these gene functions or to the bad condition of wild-type seeds, which may distort the results. The CPK3 overexpressing line *cpk3-3* was less affected from salt stress, consistent with its role in salt-stress acclimation (Mehlmer *et al.*, 2010). Under additional K^+ deprivation, this effect was even more obvious (Fig. 3.8.1, right side). Whereas all other lines suffered from low K^+ levels under salt stress, the overexpressor *cpk3-3* displayed an unchanged germination rate. Strikingly, germination of the *tpk1* knock-out line was considerably reduced under these conditions. These data indicate that both CPK3 and TPK1 are important for K^+ homeostasis under salt stress, further strengthening our finding that CPK3 is involved in the regulation of TPK1. However, it should be noted that in case of TPK1 this result could not be confirmed by other *tpk1* knock-out or overexpressing lines due to unknown reasons (data not shown).

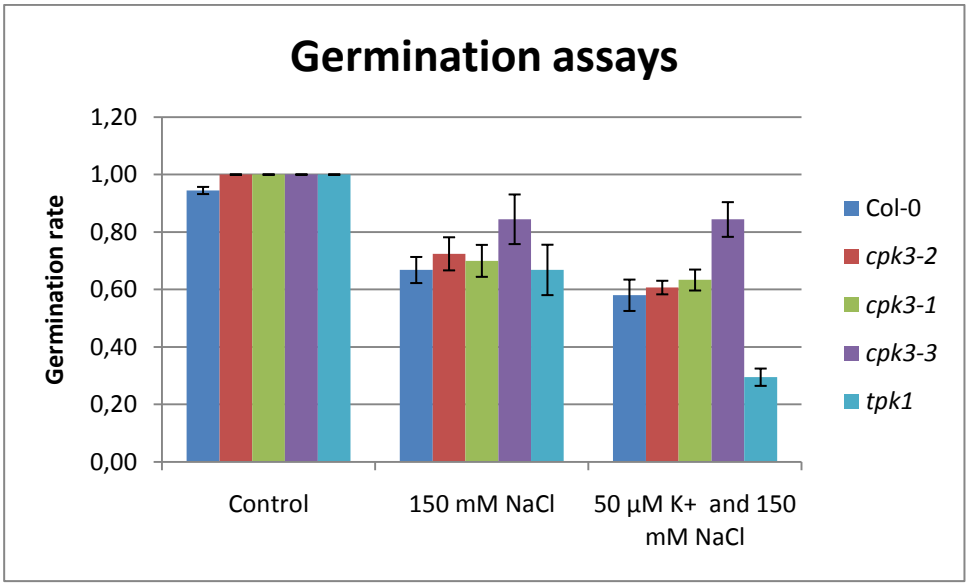

Fig. 3.8.1. Germination rates of *cpk3* and *tpk1* lines under salt stress and K^+ deprivation. Seeds were dispersed on plates with basal mineral medium supplemented with 2 mM KCl (control, left side), 150 mM NaCl and 2 mM KCl (150 mM NaCl, middle) or 150 mM NaCl and 50 µM KCl as sole source for K^+ (right side). Col-0 is the wild-type control, *cpk3-2* a *cpk3* knock-out line, *cpk3-1* a *cpk3* knock-down line, *cpk3-3* a *cpk3* overexpressing line, and *tpk1* is a *tpk1* knock-out line. Germination was scored four days after exposure to light. A seed was classified as germinated when the radicle was visible. Mean germination rates were calculated from 3 and 5 plates with approximately 100 seeds per line in case of control and stress conditions, respectively. Error bars represent the standard deviation.

4 Discussion

4.1 Subcellular Localisation of CPK3

Previous studies with GFP/YFP-fusions of CPK3 have detected CPK3 in the nucleus, at cellular membranes and in the cytosol (Mehlmer *et al.*, 2010; Dammann *et al.*, 2003). However, the extent to which CPK3 was found to be associated with membranes was controversial. In the present work, I analysed the distribution of endogenous CPK3 in wild-type plants by biochemical fractionation. Thereby, I could demonstrate that the majority of CPK3 is soluble both in roots and leaves (Fig. 3.1.1). This approach does not distinguish between soluble proteins in the cytosol and inside organelles, such as nuclear proteins, since organelles partly are disrupted during the homogenisation process. Therefore, the precise portion of cytosolic CPK3 cannot be calculated. Together with the result from transient expression of CPK3-YFP fusion proteins in tobacco leaves, however, it can be concluded that a considerable portion of CPK3 is localised in the cytosol (Fig. 3.1.2).

These results are fully consistent with the results of Dammann and co-workers (2003). In their work, microscopic analysis of roots from transgenic *Arabidopsis* plants expressing CPK3-GFP under the 35S promoter revealed a nuclear and cytosolic localisation of CPK3-GFP. Although not stated by the authors, in this report a signal from CPK3-GFP at the plasma membrane is visible as well. Moreover, the microsomal/soluble distribution of CPK3 obtained by biochemical fractionation of roots from these plants is almost identical to my results. In contrast, no signal of CPK3 in the soluble fraction of wild-type *Arabidopsis* leaves has been detected by Mehlmer and co-workers (2010). This is likely due to the fact that similar protein amounts of the soluble and microsomal fractions have been used in this experiment instead of same portions. As approximately ten times more proteins are present in the soluble fraction than in the microsomal one, the soluble fraction was strongly underrepresented in this approach, leading to distorted results.

In addition, I investigated the membrane association of CPK3 in more detail by biochemical approaches. This data from wild-type plants is highly reliable as it does not involve overexpression or manipulation of proteins, which may result in localisation artefacts. Isolation of highly pure plasma membrane by two-phase partitioning demonstrated that CPK3 is associated with the plasma membrane in leaves (Fig. 3.2.1A). Separation of membranes on sucrose densities revealed a good co-localisation of CPK3 with the vacuolar membrane in leaves, indicating that CPK3 is attached to the tonoplast in this tissue (Fig. 3.2.1B). This is consistent with the stronger signal of CPK3 in the upper phase of the two-

phase partitioning, which contains similar amounts of plasma membrane but also several endomembranes. In contrast, CPK3 did not co-migrate with the vacuolar membrane in roots but predominantly with the plasma membrane (Fig. 3.2.1C). Accordingly, a picture of the subcellular localisation of CPK3 can be drawn as follows: The majority of CPK3 is found in the cytosol and the nucleus while a smaller fraction is associated with membranes. Whereas in roots insoluble CPK3 is mostly attached to the plasma membrane, the majority of insoluble CPK3 is associated with the vacuolar membrane in leaves with a small portion at the plasma membrane.

4.2 Implications of Membrane Association for the Function of CPK3

The wide-spread subcellular localisation of CPK3 offers several possibilities for its role in the salt-stress response. The nuclear localisation suggests the involvement of CPK3 in transcriptional reprogramming by phosphorylation of transcription factors (Mehlmer *et al.*, 2010). However, a comparison of transcript levels of stress-related marker genes in wild-type, *cpk3* knock-out and overexpressing lines by RT-PCR did not reveal CPK3-dependent differences (Mehlmer *et al.*, 2010). Accordingly, the salt-sensitive phenotype of *cpk3* ko plants cannot be explained by the lack of nuclear localised CPK3 (Mehlmer *et al.*, 2010).

Another interesting aspect of the subcellular localisation of CPK3 is its membrane association. This suggests that CPK3 might be involved in phosphorylation of ion channels/transporters to maintain cellular ion homeostasis upon salt stress (Mehlmer *et al.*, 2010). Notably, a regulation of ion channels by CPK3 has been proposed previously in guard cells where CPK3 regulates S-type anion channels and Ca^{2+} permeable channels together with CPK6 (Mori *et al.*, 2006). This is consistent with the suggestion that a tight positioning of the kinase, its target, and the activating Ca^{2+} signal increases the efficiency of Ca^{2+} signal transduction (Mehlmer *et al.*, 2010). Since Ca^{2+} signals are very short-lived and spatially restricted, the membrane association might furthermore have implications for the activation of CPK3. For instance, a Ca^{2+} flux along the plasma membrane upon salt/drought stress has been reported in *Arabidopsis* seedlings, and Ca^{2+} is released from the vacuole in response to drought stress but to a lesser extent upon cold or oxidative stress (Knight *et al.*, 1997). Thus, the different localisations of CPK3 observed in roots and in leaves indicate different functions and targets of this kinase in these two organs, which is in line with the different mechanisms used by roots and leaves to cope with salt stress (Munns and Tester, 2008). To resolve the question of the relation between localisation and function of CPK3, we are

currently generating *cpk3* complementation lines expressing differentially localised CPK3s. Germination assays on medium with salt will then reveal which localisation of CPK3 is required for its function in the acclimation to salt stress.

4.3 Role of *N*-Myristoylation

Recently, it has been shown that CPK3 can be myristoylated at its N terminus and that this modification is crucial for its membrane association (Mehlmer *et al.*, 2010). Nevertheless, due to the relatively high dissociation constant of the binding of a myristoylated peptide to a phospholipid bilayer, myristoylation alone is not sufficient for stable membrane anchoring (Resh, 2006). Additional stability can be provided by a second anchor such as palmitoylation, by a basic region within the protein that electrostatically interacts with negatively charged phospholipids or by interaction with other membrane-bound proteins (Resh, 1999). However, stabilising factors have not been reported for CPK3, which also lacks a cysteine near its N terminus that could be palmitoylated. Thus, the wide-spread subcellular localisation of CPK3 may be due to the lack of stable membrane anchoring. This is particularly interesting, as CPK3 is the only CDPK in *Arabidopsis* that harbours a glycine in position two - the prerequisite for myristoylation - but does not have the aforementioned cysteine in close proximity. Due to the unstable membrane anchoring, CPK3 could shuffle between the nucleus and cytosol with transient membrane associations. The different membrane associations in roots and leaves, however, suggest a model in which the membrane association of CPK3 is at least partly stabilised by other factors such as membrane proteins. This is consistent with the observation that a CPK3-G2A mutant, which cannot be myristoylated, still shows a partial membrane association (Mehlmer *et al.*, 2010). As the protein composition of membranes in roots and leaves is not equal, the differences in stabilising factors may then lead to organ-specific membrane anchoring of CPK3.

The flexible membrane association of CPK3 could also involve a myristyl switch. This is defined as a conformational change that leads to the concealment of the fatty acid tail in a hydrophobic pocket within the protein or to the exposure of this anchor, thus reversibly affecting the membrane association of the protein (Resh, 1999). In this respect, it would be interesting to analyse whether the membrane association of CPK3 is affected by conformational changes of CPK3 upon binding to Ca^{2+} and whether such changes are observed under stress conditions.

4.4 Interaction Partners of CPK3

In the present studies, putative targets identified in a recent proteomics approach by Mehlmer and co-workers (2010) were tested for their interaction with CPK3. Interestingly, BiFC assays in tobacco epidermal cells revealed an interaction between CPK3 and a remorin protein, ERD13, PP2C-type phosphatases and a protein of unknown function, providing a first evidence for these proteins being targets of CPK3.

The remorin belongs to a gene family which is unique to plants and has 16 members in *Arabidopsis* (Raffaele *et al.*, 2007). Consistent with the results obtained from my localisation study (Fig. 3.6.1C), remorins have been repeatedly found in lipid rafts or in other plasma membrane fractions (Mongrand *et al.*, 2004; Lefebvre *et al.*, 2010; Bariola *et al.*, 2004). This is surprising, since remorins are rather hydrophilic proteins without predicted transmembrane domains that also have no membrane anchors despite potential sites for isoprenylation in some cases (Bariola *et al.*, 2004; Raffaele *et al.*, 2007). Therefore, it has been proposed by Bariola and co-workers (2004) that remorins form complexes with membrane-anchored proteins to stabilise their membrane association.

Interestingly, a remorin has recently been shown to be involved in infection with rhizobia in the legume *Medicago trancula* (Lefebvre *et al.*, 2010). As this remorin interacts with receptor-like kinases, a scaffolding function of remorins for signalling complexes at the plasma membrane has been proposed (Lefebvre *et al.*, 2010). Interestingly, the remorin used in my study is transcriptionally upregulated upon salt stress (Kreps *et al.*, 2002). Similar to the function of other remorins, this remorin could be involved in the organisation of signalling complexes in *Arabidopsis*, for instance by strengthening the attachment of CPK3 to the plasma membrane, in particular upon salt stress. Therefore, it would be interesting to investigate whether co-expression of the remorin in tobacco changes the subcellular localisation of CPK3 towards a more pronounced membrane association.

ERD13, also known as GSTF10, is a glutathione-*S*-transferase (GST) of the phi class (Dixon *et al.*, 2002). The best-characterised function of these proteins is the detoxification of herbicides by *S*-glutathionylation, which is followed by the sequestration of the conjugated products into the vacuole (Edwards *et al.*, 2000). In addition, GSTs may be involved in reduction of organic compounds after oxidative stress, since some GSTs have glutathione peroxidase activity and many are induced upon several abiotic stresses (Dixon *et al.*, 2002). Notably, ERD13 has been initially identified as a dehydration-inducible gene and is furthermore upregulated upon salt, cold and oxidative stress (Kiyosue *et al.*, 1993; Bianchi *et*

al., 2002). Moreover, an interaction between ERD13 and the brassinosteroid co-receptor BAK1 has been reported recently, suggesting the involvement of ERD13 in signalling pathways (Ryu *et al.*, 2009). The same study also revealed that ERD13 knock-down plants display a salt-sensitive phenotype, which is similar to the phenotype of *cpk3* knock-out plants (Mehlmer *et al.*, 2010) and further strengthens a functional interaction with CPK3. Accordingly, the interaction of ERD13 with CPK3 may help to reduce oxidative damage upon abiotic stresses and could also involve a new function of ERD13 as a signalling component.

PP2C and AP2C1 are PP2C-type phosphatases, of which 76 members have been identified in *A. thaliana* (Schweighofer *et al.*, 2004). AP2C1 has previously been shown to inhibit the MAP kinases MPK4 and MPK6 (Schweighofer *et al.*, 2007). Similarly, the interaction of CPK3 with these phosphatases provides a first evidence of a negative regulation of CPK3. In contrast to MAP kinases, however, no phosphorylation site crucial for kinase activity has been identified so far in CPK3, and the inhibition of autophosphorylation of Ser242 of CPK3 had only mild effects (Mehlmer, 2008).

PP2C (but not AP2C1) has been identified as a putative target of CPK3 in a phosphoproteomics approach, and phosphorylated peptides of PP2C are listed in the Phosphat 3.0 database (http://phosphat.mpimp-golm.mpg.de/db.html) (Mehlmer *et al.*, 2010). This suggests that this PP2C may also be regulated by CPK3 via phosphorylation. This hypothesis is particularly interesting as PP2Cs are monomeric enzymes the regulation of which is an enigma (Schweighofer *et al.*, 2004). Moreover, the positive or negative regulation of PP2Cs by CPK3 could provide an effective means for cross talk between signalling pathways.

The protein of unknown function interacts with CPK3 both in BiFC and yeast two-hybrid assays. Nevertheless, this interaction is likely to be an artefact since localisation studies with a C-terminally tagged protein showed a punctuate localisation (Fig. 3.6.1D), and a mitochondrial targeting is predicted by ARAMEMNON (Schwacke *et al.*, 2003). The observed interaction with CPK3 can be explained by the usage of an N-terminally tagged fusion protein, in which the natural targeting of the unknown protein is obviously masked (Fig. 3.6.1E, F). The unknown protein is homologous to another protein of unknown function in *Arabidopsis* (At1g73770). However, this protein is predicted by ARAMEMNON to be imported into the mitochondria as well and is therefore unlikely to be a target of CPK3.

4.5 Specificity of BiFC

The interactions observed with CPK3 and its putative targets could not be confirmed in yeast two-hybrid assays, except for the unknown protein and the formerly isolated transcription factor bZIP63. This discrepancy raises the question whether the BiFC assays might be too unspecific.

A major problem in BiFC is that the N- and C-terminal halves of fluorescent protein display an intrinsic self-association. The association constants vary for different combinations, but in general a strong fluorescent intensity correlates with higher association rates, increasing unspecific signals (Kerppola, 2009). In the present study, I used split fluorescent proteins that have relatively small self-association rates among those with enhanced fluorescent intensity (Waadt *et al.*, 2008). However, also in cases of obviously weak interaction with CPK3 a fluorescent signal was obtained by opening the detector gain and the pinhole of the microscope (Fig. 3.3.2). No signal was only detected when one protein was not expressed (e.g. SOS1, data not shown). The increase in fluorescent signal resulted in background haze and visible signals from chlorophyll autofluorescence, but this is not easy to detect for inexperienced users. Accordingly, the obtained fluorescence should be compared with a positive control to distinguish between specific and unspecific signals. In case of CPK3 and TPK1, mutational analysis was used to demonstrate that the observed signals in fact arise from interaction between these proteins (Fig. 3.7.1). Moreover, stringent microscopy settings were generally used in BiFC assays. The fact that under these conditions no fluorescent signal was obtained in case of calreticulin 1 and 2 and KAB1 (Fig. 3.3.2 and data not shown) underpins that strong fluorescent signals are not only due to co-localisation by any chance. Thus, under stringent conditions BiFC specifically detects protein interactions *in vivo*.

However, it remains to be elucidated why most of the interactions were not observed in the yeast two-hybrid assay. It should be noted that yeast two-hybrid screens and assays with CDPKs have successfully been applied only in rare cases, e.g. for AtCPK11 (Rodriguez Milla *et al.*, 2006). The interaction between CPK3 and the unknown protein is the strongest interaction observed in yeast with CPK3 so far. Compared to others, however, this interaction is extremely weak. For instance, dimerisation of bZIP63 or interactions of bZIP63 with AKIN10 resulted in approximately 30 or 10 times greater β-galactosidase activities, respectively (data not shown). Typically enough, the soluble N-terminus of TPK1 containing the CDPK phosphorylation site does not interact with CPK3 in yeast either

(Mehlmer, 2008) and no good interaction partner of CPK3 has been identified in any yeast two-hybrid screen (M. Teige, unpublished data).

One reason for this could be that the C-terminal autoinhibitory domain of CPK3 may be required for interaction with its targets. However, this domain has to be deleted in order to compensate the lack of appropriate Ca^{2+} signals in yeast, which would generally abolish any interaction otherwise. The used CPK3 construct might also be only weakly expressed in yeast. One reason may be differences in codon usage between yeast and *Arabidopsis*, since the usage of rare codons impedes the translation of the corresponding mRNA (Daly and Hearn, 2005). Notably, the used sequence of CPK3 contains 26 codons used in 14% or less for an individual amino acid in yeast and 12 of these are extremely rare with usages from 4% to 7% (*Saccharomyces cerevisiae* codon usage tables from ftp://genome-ftp.stanford.edu/pub/codon/ysc.orf.cod). However, the possibility of a weakly expressed CPK3 has never been tested since no appropriate antibody for this CPK3 construct is available. Together, these facts strongly suggest that yeast-two hybrid assays may not be the appropriate means to detect interactions between CPK3 and its targets.

In any case, the interactions observed in BiFC need to be further evaluated. First, it should be investigated whether these proteins can be phosphorylated by CPK3 in *in-vitro* kinase assays. Furthermore, corresponding knock-out and overexpressor lines should be obtained or generated and analysed for CPK3-related phenotypes. In the long term, stable transgenic lines expressing tagged versions of these proteins would be a great help to study the function of these proteins without having antibodies specific for the individual proteins.

4.6 Interaction of CPK3 with TPK1 and Its Physiological Function

In the present work, I used BiFC to demonstrate that CPK3 interacts with TPK1, a vacuolar K^+ channel, *in planta*, and that this interaction involves arginines close to the 14-3-3 binding site of TPK1 (Figs. 3.3.2, 3.7.1). Moreover, I showed that both CPK3 and TPK1 are involved in K^+ homeostasis upon salt stress (Fig. 3.8.1), indicating a functional relation between these proteins. Together with the finding that TPK1 is phosphorylated by CPK3 *in vitro* (Mehlmer, 2008), this data suggests that CPK3 phosphorylates TPK1 *in vivo*.

Using a TPK1 mutant in which Ser42 in the 14-3-3 binding motif was replaced by Ala, it has been shown that CPK3 exclusively phosphorylates this residue in the N terminus of TPK1 (Latz *et al.*). A phosphorylation of Ser42 was furthermore shown to be required for binding of the 14-3-3 binding protein GRF8, which activates TPK1 and stimulates K^+ fluxes across

the tonoplast (Latz *et al.*, 2007). Thus, the phosphorylation of TPK1 by CPK3 most likely results in activation of TPK1.

CPK3 is likely not to be the only CDPK involved in regulation of TPK1, since also CPK4, CPK5, CPK12 and CPK29 interact with TPK1 in BiFC and phosphorylate TPK1 *in vitro* (Latz *et al.*, Bernhard Wurzinger and own unpublished data). However, it remains unclear whether all these interactions have an *in-vivo* function. For instance, CPK29 may not phosphorylate TPK1 immediately after the sensing of salt stress, as its transcription levels in the absence of stress are very low and CPK29 possibly has to be synthesised beforehand (Latz *et al.*). Subcellular localisation of CDPKs might provide specificity as well. In case of Ca^{2+}-regulated kinases, the localisation does not only determine the targets likely to be encountered but also by which Ca^{2+} signals CDPKs are activated. CPK3 is the only *Arabidopsis* CDPK found to localise to the vacuolar membrane in leaves so far. This is interesting since TPK1 binds Ca^{2+} by itself, and this binding is a prerequisite for its permeability (Latz *et al.*, 2007). It is thereby tempting to speculate that unlike to other CDPKs, CPK3 and TPK1 sense the same Ca^{2+} signals at the vacuolar membrane, allowing an activating effect of phosphorylation of TPK1 by this CDPK.

A primary function of TPK1 is the maintenance of cellular K^+ homeostasis (Gobert *et al.*, 2007). This is particularly important upon salt stress where increasing cytosolic K^+ levels are required in order to reduce the toxicity of Na^+ (Shabala, 2008; Zhu, 2003; Luan *et al.*, 2009). First, high K^+ levels in the cytosol counteract the ability of Na^+ to compete with K^+ in binding at cytosolic enzymes (Shabala, 2008). Second, release of K^+ from

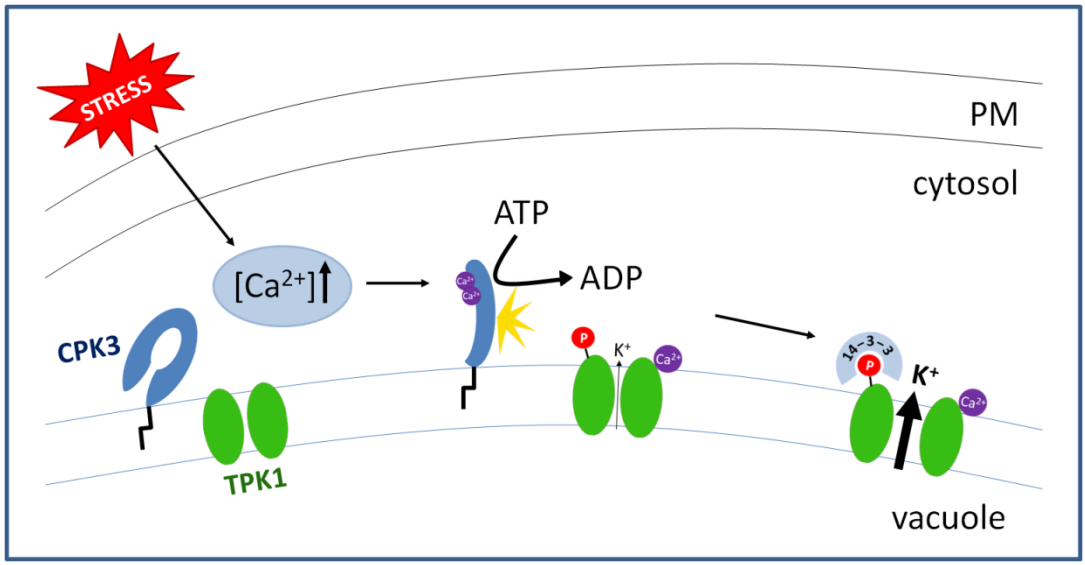

Fig. 4.6.1. Model of the regulation of TPK1 by CPK3 upon salt stress.

vacuoles allows sequestering of Na^+ into the vacuole without loss of turgor where it loses its toxic effect (Munns and Tester, 2008; Kader and Lindberg, 2010). Besides TPK1, the slow-activating vacuolar (SV) K^+ channels are regulated by the 14-3-3 protein GRF8 as well (Latz *et al.*, 2007). Interestingly, these channels are also permeable for Na^+, which is contrary to the specificity for K^+ of TPK1 (Latz *et al.*, 2007). SV channels have furthermore been shown to be negatively regulated by the 14-3-3 protein GRF8, whereas TPK1 is activated by this 14-3-3 protein (Latz *et al.*, 2007). Accordingly, it has been proposed that regulation of vacuolar ion channels by 14-3-3 proteins may abolish the passive efflux of Na^+ into the cytosol during the release of K^+, enabling the trapping of Na^+ in the vacuole and increased salt tolerance (Latz *et al.*, 2007). The kinases responsible for phosphorylation of SV channels, however, have not been identified so far.

According to our data, we present a model of the regulation of TPK1 by CPK3 (Fig. 4.6.1). Upon salt stress, Ca^{2+} signals at the vacuolar membrane activate CPK3. These signals also allow binding of Ca^{2+} by TPK1, which results in transition to an activatable state and low K^+ permeability. Active CPK3 phosphorylates TPK1 at Ser42 in the 14-3-3 binding motif. This enables the binding of the 14-3-3 protein GRF8, which in turn boosts the permeability of TPK1. TPK1 then specifically releases K^+ ions from the vacuole into the cytosol, reducing the toxic effect of Na^+. Thus, the regulation of TPK1 by CPK3 provides a mechanism that explains how CPK3 may increase the tolerance of plants towards salt stress.

5 References

Baena-Gonzalez, E. and Sheen, J. (2008) Convergent energy and stress signaling. *Trends in plant science*, **13**, 474-482.

Bariola, P.A., Retelska, D., Stasiak, A., Kammerer, R.A., Fleming, A., Hijri, M., Frank, S. and Farmer, E.E. (2004) Remorins form a novel family of coiled coil-forming oligomeric and filamentous proteins associated with apical, vascular and embryonic tissues in plants. *Plant molecular biology*, **55**, 579-594.

Benetka, W., Mehlmer, N., Maurer-Stroh, S., Sammer, M., Koranda, M., Neumuller, R., Betschinger, J., Knoblich, J.A., Teige, M. and Eisenhaber, F. (2008) Experimental testing of predicted myristoylation targets involved in asymmetric cell division and calcium-dependent signalling. *Cell cycle* **7**, 3709-3719.

Bianchi, M.W., Roux, C. and Vartanian, N. (2002) Drought regulation of GST8, encoding the Arabidopsis homologue of ParC/Nt107 glutathione transferase/peroxidase. *Physiologia plantarum*, **116**, 96-105.

Boehmer, M. and Romeis, T. (2007) A chemical-genetic approach to elucidate protein kinase function in planta. *Plant molecular biology*, **65**, 817-827.

Bouche, N., Scharlat, A., Snedden, W., Bouchez, D. and Fromm, H. (2002) A novel family of calmodulin-binding transcription activators in multicellular organisms. *The Journal of biological chemistry*, **277**, 21851-21861.

Boudsocq, M., Willmann, M.R., McCormack, M., Lee, H., Shan, L., He, P., Bush, J., Cheng, S.H. and Sheen, J. (2010) Differential innate immune signalling via Ca^{2+} sensor protein kinases. *Nature*, **464**, 418-422.

Chandran, V., Stollar, E.J., Lindorff-Larsen, K., Harper, J.F., Chazin, W.J., Dobson, C.M., Luisi, B.F. and Christodoulou, J. (2006) Structure of the regulatory apparatus of a calcium-dependent protein kinase (CDPK): a novel mode of calmodulin-target recognition. *Journal of molecular biology*, **357**, 400-410.

Cheng, S.H., Willmann, M.R., Chen, H.C. and Sheen, J. (2002) Calcium signaling through protein kinases. The Arabidopsis calcium-dependent protein kinase gene family. *Plant physiology*, **129**, 469-485.

Choi, H.I., Park, H.J., Park, J.H., Kim, S., Im, M.Y., Seo, H.H., Kim, Y.W., Hwang, I. and Kim, S.Y. (2005) Arabidopsis calcium-dependent protein kinase AtCPK32 interacts with ABF4, a transcriptional regulator of abscisic acid-responsive gene expression, and modulates its activity. *Plant physiology*, **139**, 1750-1761.

Daly, R., Hearn, M.T. (2005) Expression of heterologous proteins in Pichia pastoris: a useful experimental tool in protein engineering and production. *Journal Molecular Recognition*, **18(2)**, 119-38.

Dammann, C., Ichida, A., Hong, B., Romanowsky, S.M., Hrabak, E.M., Harmon, A.C., Pickard, B.G. and Harper, J.F. (2003) Subcellular targeting of nine calcium-dependent protein kinase isoforms from Arabidopsis. *Plant physiology*, **132**, 1840-1848.

Das, R. and Pandey, G.K. (2010) Expressional analysis and role of calcium regulated kinases in abiotic stress signaling. *Current genomics*, **11**, 2-13.

Dixon, D.P., Lapthorn, A. and Edwards, R. (2002) Plant glutathione transferases. *Genome biology*, **3**, REVIEWS3004.

Dodd, A.N., Kudla, J. and Sanders, D. (2010) The language of calcium signaling. *Annual review of plant biology*, **61**, 593-620.

Edwards, R., Dixon, D.P. and Walbot, V. (2000) Plant glutathione S-transferases: enzymes with multiple functions in sickness and in health. *Trends in plant science*, **5**, 193-198.

Finkler, A., Ashery-Padan, R. and Fromm, H. (2007) CAMTAs: calmodulin-binding transcription activators from plants to human. *FEBS letters*, **581**, 3893-3898.

Galili, G., Sengupta-Gopalan, C. and Ceriotti, A. (1998) The endoplasmic reticulum of plant cells and its role in protein maturation and biogenesis of oil bodies. *Plant molecular biology*, **38**, 1-29.

Geiger, D., Scherzer, S., Mumm, P., Marten, I., Ache, P., Matschi, S., Liese, A., Wellmann, C., Al-Rasheid, K.A., Grill, E., Romeis, T. and Hedrich, R. (2010) Guard cell anion channel SLAC1 is regulated by CDPK protein kinases with distinct Ca^{2+} affinities. *Proceedings of the National Academy of Sciences of the United States of America*, **107**, 8023-8028.

Gobert, A., Isayenkov, S., Voelker, C., Czempinski, K. and Maathuis, F.J. (2007) The two-pore channel TPK1 gene encodes the vacuolar K+ conductance and plays a role in K^+ homeostasis. *Proceedings of the National Academy of Sciences of the United States of America*, **104**, 10726-10731.

Haley, A., Russell, A.J., Wood, N., Allan, A.C., Knight, M., Campbell, A.K. and Trewavas, A.J. (1995) Effects of mechanical signaling on plant cell cytosolic calcium. *Proceedings of the National Academy of Sciences of the United States of America*, **92**, 4124-4128.

Hardin, S.C., Winter, H. and Huber, S.C. (2004) Phosphorylation of the amino terminus of maize sucrose synthase in relation to membrane association and enzyme activity. *Plant physiology*, **134**, 1427-1438.

Harper, J.F., Breton, G. and Harmon, A. (2004) Decoding Ca(2+) signals through plant protein kinases. *Annual review of plant biology*, **55**, 263-288.

Hegeman, A.D., Rodriguez, M., Han, B.W., Uno, Y., Phillips, G.N., Jr., Hrabak, E.M., Cushman, J.C., Harper, J.F., Harmon, A.C. and Sussman, M.R. (2006) A phyloproteomic characterization of in vitro autophosphorylation in calcium-dependent protein kinases. *Proteomics*, **6**, 3649-3664.

Hepler, P.K., Vidali, L. and Cheung, A.Y. (2001) Polarized cell growth in higher plants. *Annual review of cell and developmental biology*, **17**, 159-187.

Hirayama, T. and Shinozaki, K. (2010) Research on plant abiotic stress responses in the post-genome era: past, present and future. *Plant J*, **61**, 1041-1052.

Hofmann-Rodrigues, D. (2007) Calcium dependent protein kinases as regulators of developmental processes in Arabidopsis thaliana. Diploma Thesis, University of Vienna.

Horie, T., Horie, R., Chan, W.Y., Leung, H.Y. and Schroeder, J.I. (2006) Calcium regulation of sodium hypersensitivities of sos3 and athkt1 mutants. *Plant & cell physiology*, **47**, 622-633.

Hrabak, E.M., Chan, C.W., Gribskov, M., Harper, J.F., Choi, J.H., Halford, N., Kudla, J., Luan, S., Nimmo, H.G., Sussman, M.R., Thomas, M., Walker-Simmons, K., Zhu, J.K. and Harmon, A.C. (2003) The Arabidopsis CDPK-SnRK superfamily of protein kinases. *Plant physiology*, **132**, 666-680.

Huang, J.F., Teyton, L. and Harper, J.F. (1996) Activation of a Ca(2+)-dependent protein kinase involves intramolecular binding of a calmodulin-like regulatory domain. *Biochemistry*, **35**, 13222-13230.

Huber, S.C., Huber, J.L., Liao, P.C., Gage, D.A., McMichael, R.W., Jr., Chourey, P.S., Hannah, L.C. and Koch, K. (1996) Phosphorylation of serine-15 of maize leaf sucrose synthase. Occurrence in vivo and possible regulatory significance. *Plant physiology*, **112**, 793-802.

Ishida, S., Yuasa, T., Nakata, M. and Takahashi, Y. (2008) A tobacco calcium-dependent protein kinase, CDPK1, regulates the transcription factor REPRESSION OF SHOOT GROWTH in response to gibberellins. *The Plant cell*, **20**, 3273-3288.

Ito, T., Nakata, M., Fukazawa, J., Ishida, S. and Takahashi, Y. (2010) Alteration of substrate specificity: the variable N-terminal domain of tobacco Ca(2+)-dependent protein kinase is important for substrate recognition. *The Plant cell*, **22**, 1592-1604.

Jia, X.Y., He, L.H., Jing, R.L. and Li, R.Z. (2009) Calreticulin: conserved protein and diverse functions in plants. *Physiologia plantarum*, **136**, 127-138.

Kader, M.A. and Lindberg, S. (2010) Cytosolic calcium and pH signaling in plants under salinity stress. *Plant signaling & behavior*, **5**, 233-238.

Kanchiswamy, C.N., Takahashi, H., Quadro, S., Maffei, M.E., Bossi, S., Bertea, C., Zebelo, S.A., Muroi, A., Ishihama, N., Yoshioka, H., Boland, W., Takabayashi, J., Endo, Y., Sawasaki, T. and Arimura, G. (2010) Regulation of Arabidopsis defense responses against Spodoptera littoralis by CPK-mediated calcium signaling. *BMC plant biology*, **10**, 97.

Kerppola, T.K. (2009) Visualization of molecular interactions using bimolecular fluorescence complementation analysis: characteristics of protein fragment complementation. *Chemical Society reviews*, **38**, 2876-2886.

Kiegle, E., Moore, C.A., Haseloff, J., Tester, M.A. and Knight, M.R. (2000) Cell-type-specific calcium responses to drought, salt and cold in the Arabidopsis root. *Plant J*, **23**, 267-278.

Knight, H., Trewavas, A.J. and Knight, M.R. (1997) Calcium signalling in Arabidopsis thaliana responding to drought and salinity. *Plant J*, **12**, 1067-1078.

Kobayashi, M., Ohura, I., Kawakita, K., Yokota, N., Fujiwara, M., Shimamoto, K., Doke, N. and Yoshioka, H. (2007) Calcium-dependent protein kinases regulate the production of reactive oxygen species by potato NADPH oxidase. *The Plant cell*, **19**, 1065-1080.

Kosuta, S., Hazledine, S., Sun, J., Miwa, H., Morris, R.J., Downie, J.A. and Oldroyd, G.E. (2008) Differential and chaotic calcium signatures in the symbiosis signaling pathway of legumes. *Proceedings of the National Academy of Sciences of the United States of America*, **105**, 9823-9828.

Kreps, J.A., Wu, Y., Chang, H.S., Zhu, T., Wang, X. and Harper, J.F. (2002) Transcriptome changes for Arabidopsis in response to salt, osmotic, and cold stress. *Plant physiology*, **130**, 2129-2141.

Kudla, J., Batistic, O. and Hashimoto, K. (2010) Calcium signals: the lead currency of plant information processing. *The Plant cell*, **22**, 541-563.

Kushwaha, R., Singh, A. and Chattopadhyay, S. (2008) Calmodulin7 plays an important role as transcriptional regulator in Arabidopsis seedling development. *The Plant cell*, **20**, 1747-1759.

Larrson, C., Sommarin, M. and Widell, S. (1994) Isolation of Highly Purified Plant Plasma Membranes and Separation of Inside-Out and Right-Side-Out Vesicles. *Methods in enzymology*, **228**, 451-469.

Latz, A., Becker, D., Hekman, M., Muller, T., Beyhl, D., Marten, I., Eing, C., Fischer, A., Dunkel, M., Bertl, A., Rapp, U.R. and Hedrich, R. (2007) TPK1, a Ca(2+)-regulated Arabidopsis vacuole two-pore K(+) channel is activated by 14-3-3 proteins. *Plant J*, **52**, 449-459.

Latz, A., Mehlmer, N., Müller, T., Zapf, S., Csaszar, E., Hedrich, R., Teige, M., Becker, D. Salt stress triggers CDPK dependent phosphorylation of the *Arabidopsis* vacuolar K^+ channel TPK1. *The plant cell* (in revision)

Lefebvre, B., Timmers, T., Mbengue, M., Moreau, S., Herve, C., Toth, K., Bittencourt-Silvestre, J., Klaus, D., Deslandes, L., Godiard, L., Murray, J.D., Udvardi, M.K., Raffaele, S., Mongrand, S., Cullimore, J., Gamas, P., Niebel, A. and Ott, T. (2010) A remorin protein interacts with symbiotic receptors and regulates bacterial infection. *Proceedings of the National Academy of Sciences of the United States of America*, **107**, 2343-2348.

Li, J., Lee, Y.R. and Assmann, S.M. (1998) Guard cells possess a calcium-dependent protein kinase that phosphorylates the KAT1 potassium channel. *Plant physiology*, **116**, 785-795.

Liu, Y., Shah, K., Yang, F., Witucki, L. and Shokat, K.M. (1998) Engineering Src family protein kinases with unnatural nucleotide specificity. *Chemistry & biology*, **5**, 91-101.

Lu, S.X. and Hrabak, E.M. (2002) An Arabidopsis calcium-dependent protein kinase is associated with the endoplasmic reticulum. *Plant physiology*, **128**, 1008-1021.

Luan, S., Lan, W. and Chul Lee, S. (2009) Potassium nutrition, sodium toxicity, and calcium signaling: connections through the CBL-CIPK network. *Current opinion in plant biology*, **12**, 339-346.

Ludwig, A.A., Romeis, T. and Jones, J.D. (2004) CDPK-mediated signalling pathways: specificity and cross-talk. *Journal of experimental botany*, **55**, 181-188.

McMichael, R.W., Jr., Bachmann, M. and Huber, S.C. (1995) Spinach Leaf Sucrose-Phosphate Synthase and Nitrate Reductase Are Phosphorylated/Inactivated by Multiple Protein Kinases in Vitro. *Plant physiology*, **108**, 1077-1082.

Mehlmer, N. (2008) Ca2+ Dependent Protein Kinases in Arabidopsis thaliana. Doctoral Thesis, University of Vienna.

Mehlmer, N., Wurzinger, B., Stael, S., Hofmann-Rodrigues, D., Csaszar, E., Pfister, B., Bayer, R. and Teige, M. (2010) The Ca(2+)-dependent protein kinase CPK3 is required for MAPK-independent salt-stress acclimation in Arabidopsis. *Plant J*.

Mongrand, S., Morel, J., Laroche, J., Claverol, S., Carde, J.P., Hartmann, M.A., Bonneu, M., Simon-Plas, F., Lessire, R. and Bessoule, J.J. (2004) Lipid rafts in higher plant cells: purification and characterization of Triton X-100-insoluble microdomains from tobacco plasma membrane. *The Journal of biological chemistry*, **279**, 36277-36286.

Mori, I.C., Murata, Y., Yang, Y., Munemasa, S., Wang, Y.F., Andreoli, S., Tiriac, H., Alonso, J.M., Harper, J.F., Ecker, J.R., Kwak, J.M. and Schroeder, J.I. (2006) CDPKs CPK6 and CPK3 function in ABA regulation of guard cell S-type anion- and Ca(2+)-permeable channels and stomatal closure. *PLoS biology*, **4**, e327.

Munns, R. and Tester, M. (2008) Mechanisms of salinity tolerance. *Annual review of plant biology*, **59**, 651-681.

Obata, T., Kitamoto, H.K., Nakamura, A., Fukuda, A. and Tanaka, Y. (2007) Rice shaker potassium channel OsKAT1 confers tolerance to salinity stress on yeast and rice cells. *Plant physiology*, **144**, 1978-1985.

Raffaele, S., Mongrand, S., Gamas, P., Niebel, A. and Ott, T. (2007) Genome-wide annotation of remorins, a plant-specific protein family: evolutionary and functional perspectives. *Plant physiology*, **145**, 593-600.

Ranjan, R., Ahmed, A., Gourinath, S. and Sharma, P. (2009) Dissection of mechanisms involved in the regulation of Plasmodium falciparum calcium-dependent protein kinase 4. *The Journal of biological chemistry*, **284**, 15267-15276.

Resh, M.D. (1999) Fatty acylation of proteins: new insights into membrane targeting of myristoylated and palmitoylated proteins. *Biochimica et biophysica acta*, **1451**, 1-16.

Resh, M.D. (2006) Trafficking and signaling by fatty-acylated and prenylated proteins. *Nature chemical biology*, **2**, 584-590.

Richter, G.L., Monshausen, G.B., Krol, A. and Gilroy, S. (2009) Mechanical stimuli modulate lateral root organogenesis. *Plant physiology*, **151**, 1855-1866.

Rius, S.P., Casati, P., Iglesias, A.A. and Gomez-Casati, D.F. (2008) Characterization of Arabidopsis lines deficient in GAPC-1, a cytosolic NAD-dependent glyceraldehyde-3-phosphate dehydrogenase. *Plant physiology*, **148**, 1655-1667.

Rodriguez Milla, M.A., Uno, Y., Chang, I.F., Townsend, J., Maher, E.A., Quilici, D. and Cushman, J.C. (2006) A novel yeast two-hybrid approach to identify CDPK substrates: characterization of the interaction between AtCPK11 and AtDi19, a nuclear zinc finger protein. *FEBS letters*, **580**, 904-911.

Romeis, T., Ludwig, A.A., Martin, R. and Jones, J.D. (2001) Calcium-dependent protein kinases play an essential role in a plant defence response. *The EMBO journal*, **20**, 5556-5567.

Ryu, H.Y., Kim, S.Y., Park, H.M., You, J.Y., Kim, B.H., Lee, J.S. and Nam, K.H. (2009) Modulations of AtGSTF10 expression induce stress tolerance and BAK1-mediated cell death. *Biochemical and biophysical research communications*, **379**, 417-422.

Saijo, Y., Hata, S., Kyozuka, J., Shimamoto, K. and Izui, K. (2000) Over-expression of a single Ca2+-dependent protein kinase confers both cold and salt/drought tolerance on rice plants. *Plant J*, **23**, 319-327.

Sanders, D., Brownlee, C. and J.F., H. (1999) Communicating with Calcium. *The Plant cell*, **11**, 691-706.

Santoni, V. (2007) Plant plasma membrane protein extraction and solubilization for proteomic analysis. *Methods in molecular biology (Clifton, N.J*, **355**, 93-109.

Schwacke, R., Schneider, A., van der Graaff, E., Fischer, K., Catoni, E., Desimone, M., Frommer, W.B., Flugge, U.I. and Kunze, R. (2003) ARAMEMNON, a novel database for Arabidopsis integral membrane proteins. *Plant physiology*, **131**, 16-26.

Schweighofer, A., Hirt, H. and Meskiene, I. (2004) Plant PP2C phosphatases: emerging functions in stress signaling. *Trends in plant science*, **9**, 236-243.

Schweighofer, A., Kazanaviciute, V., Scheikl, E., Teige, M., Doczi, R., Hirt, H., Schwanninger, M., Kant, M., Schuurink, R., Mauch, F., Buchala, A., Cardinale, F. and Meskiene, I. (2007) The PP2C-type phosphatase AP2C1, which negatively regulates MPK4 and MPK6, modulates innate immunity, jasmonic acid, and ethylene levels in Arabidopsis. *The Plant cell*, **19**, 2213-2224.

Shabala, S. and Cuin, T.A. (2008) Potassium transport and plant salt tolerance. *Physiologia plantarum*, **133**, 651-669.

Shaw, S.L. and Long, S.R. (2003) Nod factor elicits two separable calcium responses in Medicago truncatula root hair cells. *Plant physiology*, **131**, 976-984.

Shi, H., Ishitani, M., Kim, C. and Zhu, J.K. (2000) The Arabidopsis thaliana salt tolerance gene SOS1 encodes a putative Na+/H+ antiporter. *Proceedings of the National Academy of Sciences of the United States of America*, **97**, 6896-6901.

Siegel, R.S., Xue, S., Murata, Y., Yang, Y., Nishimura, N., Wang, A. and Schroeder, J.I. (2009) Calcium elevation-dependent and attenuated resting calcium-dependent abscisic acid induction of stomatal closure and abscisic acid-induced enhancement of calcium sensitivities of S-type anion and inward-rectifying K channels in Arabidopsis guard cells. *Plant J*, **59**, 207-220.

Sottosanto, J.B., Saranga, Y. and Blumwald, E. (2007) Impact of AtNHX1, a vacuolar Na+/H+ antiporter, upon gene expression during short- and long-term salt stress in Arabidopsis thaliana. *BMC plant biology*, **7**, 18.

Spalding, E.P., Hirsch, R.E., Lewis, D.R., Qi, Z., Sussman, M.R. and Lewis, B.D. (1999) Potassium uptake supporting plant growth in the absence of AKT1 channel activity: Inhibition by ammonium and stimulation by sodium. *The Journal of general physiology*, **113**, 909-918.

Sunarpi, Horie, T., Motoda, J., Kubo, M., Yang, H., Yoda, K., Horie, R., Chan, W.Y., Leung, H.Y., Hattori, K., Konomi, M., Osumi, M., Yamagami, M., Schroeder, J.I. and Uozumi, N. (2005) Enhanced salt tolerance mediated by AtHKT1 transporter-induced Na unloading from xylem vessels to xylem parenchyma cells. *Plant J*, **44**, 928-938.

Tang, H., Vasconcelos, A.C. and Berkowitz, G.A. (1996) Physical association of KAB1 with plant K+ channel alpha subunits. *The Plant cell*, **8**, 1545-1553.

Urao, T., Katagiri, T., Mizoguchi, T., Yamaguchi-Shinozaki, K., Hayashida, N. and Shinozaki, K. (1994) Two genes that encode Ca(2+)-dependent protein kinases are induced by drought and high-salt stresses in Arabidopsis thaliana. *Mol Gen Genet*, **244**, 331-340.

Vitart, V., Christodoulou, J., Huang, J.F., Chazin, W.J. and Harper, J.F. (2000) Intramolecular activation of a Ca(2+)-dependent protein kinase is disrupted by insertions in the tether that connects the calmodulin-like domain to the kinase. *Biochemistry*, **39**, 4004-4011.

Waadt, R., Schmidt, L.K., Lohse, M., Hashimoto, K., Bock, R. and Kudla, J. (2008) Multicolor bimolecular fluorescence complementation reveals simultaneous formation of alternative CBL/CIPK complexes in planta. *Plant J*, **56**, 505-516.

Webb, A.A.R., McAinsh, M.R., Taylor, J.E. and Hetherington, A.M. (1996) Calicum ions as intracellular second messengers in higher plants. *Adv. Bot. Res.* , **2**, 45-96.

Wernimont, A.K., Artz, J.D., Finerty, P., Jr., Lin, Y.H., Amani, M., Allali-Hassani, A., Senisterra, G., Vedadi, M., Tempel, W., Mackenzie, F., Chau, I., Lourido, S., Sibley, L.D. and Hui, R. (2010) Structures of apicomplexan calcium-dependent protein kinases reveal mechanism of activation by calcium. *Nature structural & molecular biology*, **17**, 596-601.

Witte, C.P., Keinath, N., Dubiella, U., Demouliere, R., Seal, A. and Romeis, T. (2010) Tobacco calcium-dependent protein kinases are differentially phosphorylated in vivo as part of a kinase cascade that regulates stress response. *The Journal of biological chemistry*, **285**, 9740-9748.

Wu, W.-H., Zou, J.-J., Wei, F.-J., Ratnasekera, D. and Wang, C. (2010) Functional characterization of AtCPK10 and AtCPK8 in Arabidopsis response to drought stress. Abstract book *Plant Calcium Signaling 2010*. Münster.

Xing, T., Wang, X.J., Malik, K. and Miki, B.L. (2001) Ectopic expression of an Arabidopsis calmodulin-like domain protein kinase-enhanced NADPH oxidase activity and oxidative burst in tomato protoplasts. *Mol Plant Microbe Interact*, **14**, 1261-1264.

Xu, J., Tian, Y.S., Peng, R.H., Xiong, A.S., Zhu, B., Jin, X.F., Gao, F., Fu, X.Y., Hou, X.L. and Yao, Q.H. (2010) AtCPK6, a functionally redundant and positive regulator involved in salt/drought stress tolerance in Arabidopsis. *Planta*, **231**, 1251-1260.

Yoon, G.M., Cho, H.S., Ha, H.J., Liu, J.R. and Lee, H.S. (1999) Characterization of NtCDPK1, a calcium-dependent protein kinase gene in Nicotiana tabacum, and the activity of its encoded protein. *Plant molecular biology*, **39**, 991-1001.

Young, J.J., Mehta, S., Israelsson, M., Godoski, J., Grill, E. and Schroeder, J.I. (2006) CO(2) signaling in guard cells: calcium sensitivity response modulation, a Ca(2+)-independent phase, and CO(2) insensitivity of the gca2 mutant. *Proceedings of the National Academy of Sciences of the United States of America*, **103**, 7506-7511.

Zhang, W., Zhou, R.G., Gao, Y.J., Zheng, S.Z., Xu, P., Zhang, S.Q. and Sun, D.Y. (2009) Molecular and genetic evidence for the key role of AtCaM3 in heat-shock signal transduction in Arabidopsis. *Plant physiology*, **149**, 1773-1784.

Zhang, X., Ma, J. and Berkowitz, G.A. (1999) Evaluation of functional interaction between K(+) channel alpha- and beta-subunits and putative inactivation gating by Co-expression in Xenopus laevis oocytes. *Plant physiology*, **121**, 995-1002.

Zhao, Y., Franklin, R.M. and Kappes, B. (1994) Plasmodium falciparum calcium-dependent protein kinase phosphorylates proteins of the host erythrocytic membrane. *Molecular and biochemical parasitology*, **66**, 329-343.

Zhu, J.K. (2003) Regulation of ion homeostasis under salt stress. *Current opinion in plant biology*, **6**, 441-445.

Curriculum Vitae

Personal information

Name	Barbara Pfister
Date of birth	16.04.1985
Place of birth	Feldkirch, Austria
Nationality	Austrian
Address	Birkenweg 6, 6833 Klaus, Austria
E-mail	barbara.pfister@univie.ac.at

Education

1991 - 1995	Primary school, Klaus
1995 - 1999	High school, Bundesgymnasium Feldkirch
1999 - 2004	High school, Musikgymnasium Feldkirch
June 2004	School leaving examination, passed with distinction
2002 - 2005	Studies of Instrumental and Vocal Pedagogics at the Landeskonservatorium Feldkirch, completed with distinction
2005 - 2011	Studies of Molecular Biology at the University of Vienna with emphasis on biochemistry, plant biology and molecular medicine
Nov. 2009 - Nov. 2010	Diploma thesis at the Department of Biochemistry and Cell Biology at the Max F. Perutz Laboratories (MFPL) in Vienna in the research group of Markus Teige

Professional activities

April 2010	Tutorship in the practical course “Molekulare Biologie Übungen IIA” at the University of Vienna
August 2010	Conference “Plant Calcium Signaling” in Münster, Germany
Sept. 2010	Poster presentation at the “Trinational Arabidopsis Meeting” in Salzburg, Austria
2010	Successful application for the international MFPL PhD program

List of Publications

Mehlmer, N., Wurzinger, B., Stael, S., Hofmann-Rodrigues, D., Csaszar, E., Pfister, B., Bayer, R., Teige, M. (2010) The Ca^{2+}-dependent protein kinase CPK3 is required for MAPK-independent salt-stress acclimation in Arabidopsis. *The plant journal* **63**, 484-498;

Wurzinger, B., Mair, A., Pfister, B., Teige, M. Cross-talk of calcium-dependent protein kinase and MAP kinase signalling. *Plant signaling & behaviour* (accepted)

Latz, A., Mehlmer, N., Müller, T., Zapf, S., Csaszar, E., Hedrich, R., Teige, M., Becker, D. Salt stress triggers CDPK dependent phosphorylation of the *Arabidopsis* vacuolar K^+ channel TPK1. *The plant cell* (In revision; I was not author of the original manuscript but will be included in its revised form)